oligodendrocyte cell spreading and CNS myelination. *J. Cell Biol.*, **163**, 397–408.
14. Wagner, W.J., Chang, A.C., Owens, J., Hong, M.J., Brooks, A. and Coligan, J.E. (2000) Aberrant development of thymocytes in mice lacking laminin-2. *Dev. Immunol.*, **7**, 179–193.
15. Pillers, D.A., Kempton, J.B., Duncan, N.M., Pang, J., Dwinnel, S.J. and Trune, D.R. (2002) Hearing loss in the laminin-deficient dy mouse model of congenital muscular dystrophy. *Mol. Genet. Metab.*, **76**, 217–224.
16. Hartigan-O'Connor, D. and Chamberlain, J.S. (2000) Developments in gene therapy for muscular dystrophy. *Microsc. Res. Tech.*, **48**, 223–238.
17. Tinsley, J.M., Potter, A.C., Phelps, S.R., Fisher, R., Ticket, J.I. and Davies, K.E. (1996) Amelioration of the dystrophic phenotype of *mdx* mice using a truncated utrophin transgene. *Nature*, **384**, 349–353.
18. Patton, B., Miner, J.H., Chiu, A. and Sanes, J.R. (1997) Distribution and function of laminins in the neuromuscular system of developing, adult, and mutant mice. *J. Cell Biol.*, **15**, 1507–1521.
19. Noakes, P.G., Gautam, M., Mudd, J., Cunningham, J.M., Sanes, J.R. and Merlie, J.P. (1995) The renal glomerulus of mice lacking s-laminin/laminin β2 chain: nephrosis despite molecular compensation by laminin β1. *Nat. Genet.*, **10**, 400–406.
20. Miner, J.H., Cunningham, J. and Sanes, J.R. (1998) Roles for laminin in embryogenesis: exencephaly, sydactyly, and placentopathy in mice lacking the laminin α5 chain. *J. Cell Biol.*, **143**, 1713–1723.
21. Falk, M., Ferletta, M., Forsberg, E. and Ekblom, P. (1999) Restricted distribution of laminin α1 chain in normal adult mouse tissues. *Matrix Biol.*, **18**, 557–568.
22. Virtanen, I., Gullberg, D., Rissanen, J., Kivilaakso, E., Kiviluoto, T., Laitinen, L.A., Lehto. V.P. and Ekblom, P. (2000) Laminin α1-chain shows a restricted distribution in epithelial basement membranes of fetal and adult human tissues. *Exp. Cell Res.*, **257**, 298–309.
23. Miner, J.H., Lewis, R.M. and Sanes, J.R. (1995) Molecular cloning of a novel laminin chain, α5, and widespread expression in adult mouse tissues. *J. Biol. Chem.*, **270**, 28523–28526.
24. Kühl, U., Öcalan, M., Timpl, R. and von der Mark, K. (1986) Role of laminin and fibronectin in selecting myogenic versus fibrogenic cells from skeletal muscles *in vitro*. *Dev. Biol.*, **93**, 344–354.
25. Mayer, U. (2003) Integrins: redundant or important players in skeletal muscle? *J. Biol. Chem.*, **278**, 14587–14590.
26. Talts, J.F., Andac, Z., Gohring, W., Brancaccio, A. and Timpl, R. (1999) Binding of the G domains of laminin α1 and α2 chains and perlecan to heparin, sulfatides, α-dystroglycan and several extracellular matrix proteins. *EMBO J.*, **18**, 863–870.
27. Schuler, F. and Sorokin, L.M. (1995) Expression of laminin isoforms in mouse myogenic cells *in vitro* and *in vivo*. *J. Cell Sci.*, **108**, 3795–3805.
28. Vachon, P.H., Loechel, F., Xu, H., Wewer, U.M. and Engvall, E. (1996) Merosin and laminin in myogenesis: specific requirements for merosin in myotube stability and survival. *J. Cell Biol.*, **134**, 1483–1497.
29. Niwa, H., Yamamura, K. and Miyazaki, J. (1991) Efficient selection for high-expression transfectants with a novel eukaryotic vector. *Gene*, **108**, 193–200.
30. Tiger, C.F. and Gullberg, D. (1997) Absence of laminin α1 chain in the skeletal muscle of dystrophic *dy/dy* mice. *Muscle Nerve*, **20**, 1515–1524.
31. Moll, J., Barzaghi, P., Lin, S., Bezakova, G., Lochmuller, H., Engvall, E., Muller, U. and Ruegg, M.A. (2001) An agrin minigene rescues dystrophic symptoms in a mouse model for congenital muscular dystrophy. *Nature*, **413**, 302–307.
32. Michelson, A.M., Russel, E. and Harman, P.J. (1955) Dystrophia muscularis: a hereditary primary myopathy in the house mouse. *Proc. Natl Acad. Sci. USA*, **41**, 1079–1084.
33. Cohn, R.D., Herrmann, R, Wewer, U.M. and Voit, T. (1997) Changes of laminin β2 chain expression in congenital muscular dystrophy. *Neuromuscul. Disord.*, **7**, 373–378.
34. Ferletta, M., Kikkawa, Y., Yu, H., Talts, J.F., Durbeej, M., Sonnenberg, A., Timpl, R., Campbell, K.P., Ekblom, P. and Genersch, E. (2003) Opposing roles of integrin α6Aβ1 and dystroglycan in laminin-mediated extracellular signal-regulated kinase activation. *Mol. Biol. Cell*, **14**, 2088–2103.
35. Connolly, A.M., Keeling, R.M., Mehta, S., Pestronk, A. and Sanes, J.R. (2001) Three mouse models of muscular dystrophy: the natural history of strength and fatigue in dystrophin-, dystrophin/utrophin-, and laminin α2 deficient mice. *Neuromuscul. Disord.*, **11**, 703–712.
36. Cossu, G. and Mavilio, F. (2000) Myogenic stem cells for the therapy of primary myopathies: wishful thinking or therapeutic perspective? *J. Clin. Invest.*, **105**, 1669–1674.
37. Ringelman, B., Röder, C., Hallmann, R., Maley, M., Davies, M., Grounds, M. and Sorokin, L.M. (1999) Expression of laminin α1, α2, α4, and α5 chains, fibronectin, and tenascin-C in skeletal muscle of dystrophic 129ReJ *dy/dy* mice. *Exp. Cell Res.*, **246**, 165–182.
38. Nakagawa, M., Miyagoe-Suzuki, Y., Ikezoe, K., Miyata, Y., Nonaka, I., Harii, K. and Takeda, S. (2001) Schwann cell myelination occurred without basal lamina formation in laminin α2 chain-null mutant (*dy3K/dy3K*) mice. *Glia*, **35**, 101–110.
39. Bradley, W.G. and Jenkinson, M. (1975) Abnormalities of peripheral nerves in murine muscular dystrophy. *J. Neurol. Sci.*, **18**, 227–247.
40. Shorer, Z., Philpot, J., Muntoni, F., Sewry, C. and Dubowitz, V. (1995) Demyelinating peripheral neuropathy in merosin-deficient congenital muscular dystrophy. *J. Child Neurol.*, **10**, 472–475.
41. Öcalan, M., Goodman, S.L., Kühl, U., Hauschka, S.D. and von der Mark, K. (1988) Laminin alters cell shape and stimulates motility and proliferation of murine skeletal myoblasts. *Dev. Biol.*, **125**, 58–67.
42. Durbeej, M. and Campbell, K.P. (2002) Muscular dystrophies involving the dystrophin–glycoprotein complex: an overview of current mouse models. *Curr. Opin. Genet. Dev.*, **12**, 349–361.
43. DelloRusso, C., Scott, J.M., Hartigan-O'Connor, D., Salvatori, G., Barjot, C., Robinson, A.S., Crawford, R.W., Brooks, S.V. and Chamberlain, J.S. (2002) Functional correction of adult *mdx* mouse muscle using gutted adenoviral vectors expressing full-length dystrophin. *Proc. Natl Acad. Sci. USA*, **99**, 12979–12984.
44. Li, X., Talts, U., Talts, J.F., Arman, E., Ekblom, P. and Lonai, P. (2001) Akt/PKB regulates laminin and collagen IV isotypes of the basement membrane. *Proc. Natl Acad. Sci. USA*, **98**, 14416–14421.
45. Lawlor, M.A. and Alessi, D.R. (2001) PKB/Akt: a key mediator of cell proliferation, survival and insulin responses? *J. Cell Sci.*, **114**, 2903–2910.
46. Niimi, T., Hayashi, Y. and Sekiguchi, K. (2003) Identification of an upstream enhancer in the mouse laminin α1 gene defining its high level of expression in parietal endoderm cells. *J. Biol. Chem.*, **278**, 9332–9338.
47. Previtali, S.C., Nodari, A., Taveggia, C., Pardini, C., Dina, G., Villa, A., Wrabetz, L., Quattrini, A. and Feltri, M.L. (2003) Expression of laminin receptors in schwann cell differentiation: evidence for distinct roles. *J. Neurosci.*, **23**, 5520–5530.
48. Yuasa, K., Fukumoto, S., Kamasaki, Y., Yamada, A., Fukumoto, E., Kanaoka, K., Saito, K., Harada, H., Arikawa-Hirasawa, E., Miyagoe-Suzuki, Y. *et al.* (2004) Laminin α2 is essential for odontoblast differentiation regulating dentin sialoprotein expression. *J. Biol. Chem.*, **279**, 10286–10292.
49. Yurchenco, P.D., Quan, Y., Colognato, H., Mathus, T., Harrison, D., Yamada, Y. and O'Rear, J.J. (1997) The α chain of laminin-1 is independently secreted and drives secretion of its β- and γ-chain partners. *Proc. Natl Acad. Sci. USA*, **16**, 10189–10194.
50. Kadoya, Y., Kadoya, K., Durbeej, M., Holmvall, K., Sorokin, L. and Ekblom, P. (1995) Antibodies against domain E3 of laminin-1 and integrin α6 subunit perturb branching epithelial morphogenesis of submandibular glands but by different modes. *J. Cell Biol.*, **129**, 521–534.
51. Sasaki, T., Mann, K., Miner, J.H., Miosge, N. and Timpl, R. (2002) Domain IV of mouse laminin β1 and β2 chains. *Eur. J. Biochem.*, **269**, 431–442.

Available online at www.sciencedirect.com
SCIENCE DIRECT
Experimental Cell Research 296 (2004) 245–255
Experimental Cell Research
www.elsevier.com/locate/yexcr

Purification and cell-surface marker characterization of quiescent satellite cells from murine skeletal muscle by a novel monoclonal antibody

So-ichiro Fukada,[a] Saito Higuchi,[a] Masashi Segawa,[a] Ken-ichi Koda,[a] Yukiko Yamamoto,[a] Kazutake Tsujikawa,[a] Yasuhiro Kohama,[a] Akiyoshi Uezumi,[b] Michihiro Imamura,[b] Yuko Miyagoe-Suzuki,[b] Shin'ichi Takeda,[b] and Hiroshi Yamamoto[a,*]

[a] *Department of Immunology, Graduate School of Pharmaceutical Sciences, Osaka University, Suita, Osaka 565-0871, Japan*
[b] *Department of Molecular Therapy, National Institute of Neuroscience, National Center of Neurology and Psychiatry, Kodaira, Tokyo 187-8502, Japan*

Received 10 November 2003; received in revised form 16 February 2004

Available online 25 March 2004

Abstract

A novel monoclonal antibody, SM/C-2.6, specific for mouse muscle satellite cells was established. SM/C-2.6 detects mononucleated cells beneath the basal lamina of skeletal muscle, and the cells co-express M-cadherin. Single fiber analyses revealed that M-cadherin$^+$ mononucleated cells attaching to muscle fibers are stained with SM/C-2.6. SM/C-2.6$^+$ cells, which were freshly purified by FACS from mouse skeletal muscle, became MyoD$^+$ in vitro in proliferating medium, and the cells differentiated into desmin$^+$ and nuclear-MyoD$^+$ myofibers in vitro when placed under differentiation conditions. When the sorted cells were injected into *mdx* mouse muscles, donor cells differentiated into muscle fibers. Flow cytometric analyses of SM/C-2.6$^+$ cells showed that the quiescent satellite cells were c-kit$^-$, Sca-1$^-$, CD34$^+$, and CD45$^-$. More, SM/C-2.6$^+$ cells were barely included in the side population but in the main population of cells in Hoechst dye efflux assay. These results suggest that SM/C-2.6 identifies and enriches quiescent satellite cells from adult mouse muscle, and that the antibody will be useful as a powerful tool for the characterization of cellular and molecular mechanisms of satellite cell activation and proliferation.

Keywords: Cell surface marker; Satellite cell; Skeletal muscle; Stem cell

Introduction

During the last decade, many reports have described the existence of tissue-specific stem cells that are able to self-renew and generate committed progenitors. Hematopoietic stem cells in bone marrow are well-characterized and defined as c-kit$^+$, Sca-1$^+$, and Lin$^-$ [1,2], and bone marrow transplantation is now clinically applied to various immunological and hematological disorders. In addition to hematopoietic stem cells, bone marrow contains mesenchymal stem cells that have been characterized by their ability to differentiate into various types of tissue-specific cells in both in vitro and in vivo experiments. Mesenchymal stem cells can generate bone, cartilage, connective tissue [3–7], and cardiomyocytes [8]. Cord blood also contains mesenchymal stem cells [9–11] and this also forms various mesenchymal tissue cells in vitro.

It is widely accepted that the postnatal growth and repair of skeletal muscle is normally mediated by satellite cells that locate between the basal lamina and sarcolemma of myofibers [12–14]. Thus, satellite cells have been considered to be the only myogenic source for the maintenance of skeletal muscle [15,16]. Satellite cells can be enriched by culturing cells from enzymatically digested muscles [17–21]. When muscle regeneration starts, the state of the satellite cells changes from resting or quiescent to activated and proliferative. However, the conditions under which the activation and the proliferation of satellite cells are initiated have not yet been well characterized.

The myogenic potential of mesenchymal stem cells from rat bone marrow in both in vivo [22] and in vitro experiments [23] has been described. These results prompted speculation

Abbreviations: GFP-Tg, Green fluorescent protein gene transgenic; MAb, Monoclonal antibody; MP, Main population; SP, Side population; TA, Tibialis anterior.

* Corresponding author. Department of Immunology, Graduate School of Pharmaceutical Sciences, Osaka University, 1-6 Yamada-oka, Suita, Osaka 565-0871, Japan. Fax: +81-6-6879-8194.
E-mail address: hiroshiy@phs.osaka-u.ac.jp (H. Yamamoto).

0014-4827/$ - see front matter © 2004 Elsevier Inc. All rights reserved.
doi:10.1016/j.yexcr.2004.02.018

that the transplanted bone marrow cells can move to damaged muscle and grow into new muscle fibers in mice [24]. Recently, several investigators have reported that transplanted bone marrow cells participate in the muscle regeneration process in irradiated or neonatal recipient mice [25–28]. These procedures opened new pathways for tissue reconstitution therapy via cell transplantation, however, muscle fibers containing donor cell-derived markers were still too low to treat patients with primary myopathies. Very recently, Asakura et al. and others reported the possibility that other muscle stem cells, so-called side population (SP) cells, might exhibit the potential to give rise to myocytes and satellite cells in transplanted muscle [26,29,30]. Thus, the possible interchange among bone marrow cells, muscle SP cells, and satellite cells has received increasing attention from the viewpoint of understanding muscle-specific stem cell biology.

To investigate the molecular events involved in the stimulation and differentiation of satellite cells, it is important to isolate satellite cells from fresh muscles. In this report, we describe the novel monoclonal antibody, SM/C-2.6, that specifically detects satellite cells. SM/C-2.6-positive cells sorted from fresh muscle generated muscle fibers both in vitro and in vivo, and the surface phenotypes of satellite cells were defined.

Materials and methods

Animals and cells

Specific pathogen-free C3H/HeN and C57BL/6 mice aged 6 to 8 weeks were purchased from Charles River Japan (Yokohama, Japan). Specific pathogen-free *mdx* mice (of C57BL/10 background) were provided by Central Laboratories for Experimental Animals (Kanagawa, Japan). C3H/HeN newborn mice were prepared in our animal facility by brother–sister mating. Heterozygous EGFP transgenic (GFP-Tg) mice with a C57BL/6 background [31] were maintained in our animal facility by mating with normal C57BL/6 mice. Sprague–Dawley rats were purchased from CLEA Japan (Tokyo, Japan).

The mouse myogenic cell line C2/4, a subline of C2C12, was a gift from Dr. S. Yoshida (Kyoto University, Kyoto, Japan) and was maintained in culture in 10% FCS containing DMEM medium. A mouse hepatocyte cell line, NCTC1469 [32], was obtained from the Japanese Collection of Research Bioresources, National Institute of Health Sciences, Tokyo, Japan.

Freshly isolated muscle-derived cells from neonatal and adult mice were prepared according to the methods of Rando and Blau [33]. Muscles from neonatal and adult mice were isolated and digested with collagenase type II (Worthington Biochemical Corp., Lakewood, NJ) for 90 min at 37°C. We triturated muscle tissues every 15 min during 90 min incubation and passed through a 37-μm nylon mesh. Single cell suspensions were washed and stained with various mAbs. We usually obtained approximately 5×10^6 cells from 1 g of muscle of 8-week-old female C57BL/6 mice. Sorted cells were obtained from GFP-Tg mice and injected into the tibialis anterior (TA) muscles of *mdx* mice. Two weeks later, the muscles were isolated, frozen in liquid nitrogen-cooled isopentane, and cryosections were examined histologically. Cryosections were examined for GFP^+ muscle fibers under a confocal laser-scanning microscope (model MRC1024ES, Bio-Rad Laboratories, Hercules, CA).

Antibodies

A rat mAb to mouse c-kit (ACK2) [34] was a gift from Dr. S-I. Nishikawa (Kyoto University); it was labeled with FITC in our laboratory. Anti-Sca-1-PE (E13-161.7), anti-CD34-FITC (RAM34), anti-CD45-PE (30-F11), and anti-MyoD (MoAb 5.8A) were purchased from Pharmingen (San Diego, CA). A rabbit anti-mouse M-cadherin polyclonal antibody was prepared in our laboratory. A rabbit anti-mouse laminin polyclonal antibody and TRITC-conjugated goat anti-mouse immunoglobulin were purchased from LSL Co., Ltd. (Tokyo, Japan) and Chemicon International, Inc. (Temecula, CA), respectively. Rhodamine-Red TM-X conjugated goat anti-rabbit IgG and Alexa488-conjugated goat anti-rabbit IgG were purchased from Molecular Probes Inc. (Eugene, OR). A rabbit anti-desmin polyclonal antibody and FITC-conjugated goat anti-rat IgG were purchased from ICN Pharmaceuticals, Inc.-Cappel Products (Aurora, OH). Monoclonal anti-dystrophin (MANDRA-1, Sigma) was labeled with a fluorochrome Alexa 568 in our laboratory. R-PE-streptavidin (Molecular Probes) or FITC-streptavidin (Pharmingen) was used to detect biotinylated antibodies. Anti-human c-met mAb (DO-24) reactive to mouse c-met [35] was purchased from Upstate (Lake Placid, NY), and it was used with Alexa488-conjugated goat anti-mouse IgG (H+L) (Molecular Probes).

Establishment of monoclonal antibodies

MAbs were established according to a standard procedure. Briefly, $1–2 \times 10^6$ C2/4 cells were injected intraperitoneally into Sprague–Dawley rats seven times at weekly intervals. Three days after the last injection, the rats were sacrificed under ether anesthesia and splenocytes were fused with partner cells, P3X63Ag8U.1 (P3U1). Strategies for mAb selection are described in Results. Finally, a mAb clone, SM/C-2.6, was established.

Flow cytometry and cell sorting

Regular flow cytometric profiles were analyzed with a FACSCalibur analyzer and CELLQuest software (Becton Dickinson Immunocytometry Systems, Mountain View, CA). SM/C2.6-reactive mononuclear cells were fractionated on a fluorescent-activated cell sorter (EPICS Elite, Coulter Electronics, Hialeah, FL). Dead cells were excluded from

the plots based on propidium iodide staining (Sigma Co., St. Louis, MO).

Hoechst staining was performed as described by Goodell et al. (http://www.bcm.tmc.edu/genetherapy/goodell/newsite/protocols.html). In brief, hindlimb muscles of 8 week-old C57BL/6 mice were digested with collagenase type II (Worthington Biochemical), suspended at 10^6 cells per ml in Dulbecco's modified Eagle's medium (DME) (Gibco BRL, Grand Island, NY) containing 2% fetal calf serum (FCS, Boehringer-Mannheim GmbH, Mannheim, Germany), 10 mM Hepes, and 5 μg/ml Hoechst 33342 (Sigma), and incubated at 37°C for 90 min in the presence or absence of 50 μM verapamil (Sigma). After Hoechst staining, the cells were washed and stained with biotinylated-SM/C-2.6 and FITC-streptavidin (Pharmingen). Flow cytometric analyses were performed on FACSVantageSE (Becton Dickinson). Hoechst 33342 was excited with a multi-line UV laser (351.1–363.8 nm) and its fluorescence was measured with a 424/44 BP filter and 675/20 BP filter. FITC and PI were excited at 488 nm by an Ar laser, and measured with 530/30 BP and 630/22 BP filters, respectively.

Immunohistochemistry

For immunohistochemical examinations of muscles, cryosections (6 μm) were fixed in acetone for 10 min and incubated in 5% skim milk for 10 min to block nonspecific antibody binding. SM/C-2.6, anti-laminin, anti-M-cadherin, and anti-dystrophin antibodies were applied to the sections for 60 min at 37°C. SM/C-2.6 mAb was detected by FITC-conjugated goat anti-rat IgG as a second antibody. Anti-laminin and anti-M-cadherin antibodies were detected by Rhodamine Red TM-X conjugated goat anti-rabbit IgG. The signals were recorded photographically using an Axiophot microscope (Carl Zeiss, Oberkochen, Germany).

Isolation and immunostaining of single fibers

To detect muscle satellite cells attaching single fibers with SM/C-2.6 and M-cadherin, muscle fibers from extensor digitorium longus (EDL) muscles of C3H/HeN mice were prepared essentially according to the methods of Bischoff [17] and Rosenblatt et al. [18]. Briefly, dissected muscle was incubated with 0.5% type I collagenase (Worthington) in DME at 37°C for 90 min. The muscle mass was transferred to fresh growth medium, high-glucose DME containing 10% FCS and penicillin (200 U/ml)–streptomycin (200 μg/ml) (Gibco BRL). The muscle mass was then triturated with a fire-polished wide-mouth Pasteur pipette. Fibers were transferred to a Matrigel (Collaborative Biomedical, Bedford, MA)-coated Lab-Tek chamber (Nalge Nunc International, Naperville, IL) and fixed in 4% paraformaldehyde in PBS for 5 min at room temperature. Fibers were permeabilized with 0.5% Triton X-100 (Nacalai Tesque, Kyoto, Japan) in PBS at room temperature for 20 min, then the nonspecific binding was blocked by incubation with 5% skim milk (in PBS) for 10 min. SM/C-2.6 and anti-M-cadherin antibodies were applied for 60 min at 37°C. Antibodies were detected using the second antibodies described in the earlier section.

Immunostaining of cultured cells

SM/C-2.6-reactive cells were fractionated on a cell sorter (EPICS Elite, Coulter Electronics), cultured, and then fixed with 2% PFA in PBS at room temperature for 10 min. Cells were permeabilized with 0.25% Triton X-100 in PBS at room temperature and then incubated in 5% skim milk for 10 min. Anti-MyoD and anti-desmin antibodies were added for 60 min at 37°C. Anti-MyoD mAb was detected using TRITC-conjugated goat anti-mouse IgG, and anti-desmin antibody was detected by Alexa 488-conjugated goat anti-rabbit IgG.

Results

Novel monoclonal antibody SM/C-2.6 detects skeletal muscle satellite cells

Satellite cell-specific mAbs were screened in three successive steps. First, mAbs that reacted to C2/4 (C2C12) immunogen were selected by flow cytometry. Second, mAbs that stained mouse thymocytes were discarded to exclude clones reactive to common mouse antigens. At this step, clones reactive to most mouse bone marrow cells were also discarded. Last, the clones reactive to mononuclear cells beneath the basal lamina of mouse skeletal muscles were selected immunohistochemically, and finally, we established the mAb SM/C-2.6. Flow cytometric data show that SM/C-2.6 stains C2/4 (Fig. 1Aa) and a fraction of bone marrow cells (approximately 10%) (Fig. 1Ac), but not thymocytes (Fig. 1Ab). SM/C-2.6 detects mononuclear cells residing beneath the laminin-positive basal lamina of muscle (Figs. 1Ba–c). This is the typical position at which muscle satellite cells reside. SM/C-2.6-positive cells (Fig. 1Bd) were also stained by M-cadherin (Fig. 1Be), which is a typical marker molecule for satellite cells. To confirm that the cells were satellite cells, we isolated living single fibers and stained them with SM/C-2.6. SM/C-2.6-stained mononuclear cells on freshly isolated single fibers. The SM/C-2.6-positive cells attached to a single fiber (Fig. 1Bg) were also stained by M-cadherin (Fig. 1Bh). The myonuclei visualized by counterstaining with DAPI expressed neither SM/C-2.6 nor M-cadherin (Fig. 1Bi).

SM/C-2.6-positive cells differentiate to myoblasts and myotubes in vitro

To determine whether SM/C-2.6-positive cells express other muscle-related molecules, we next fractionated the

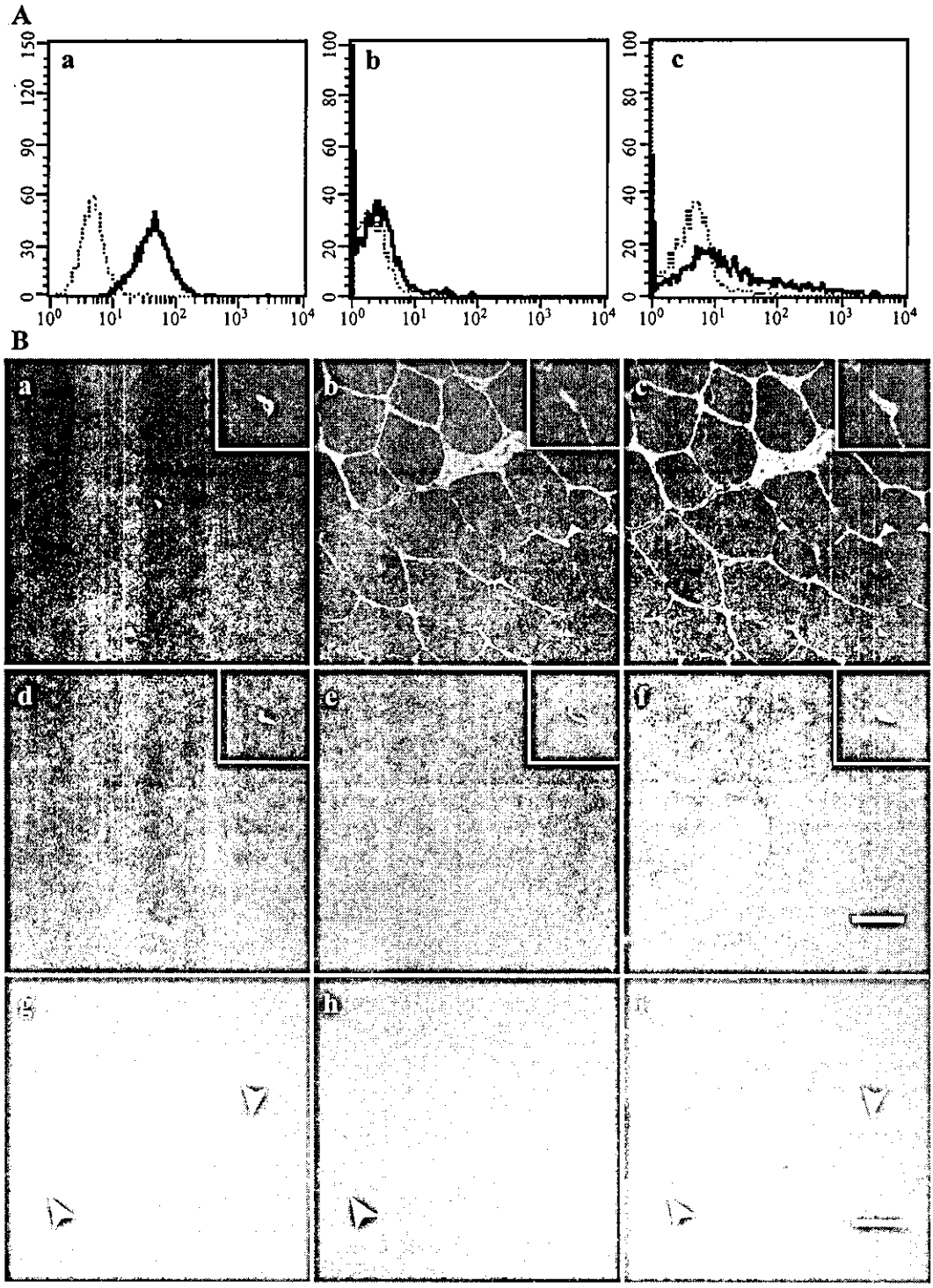

Fig. 1. Establishment of a novel monoclonal antibody, SM/C-2.6. A: SM/C-2.6 reacts with C2/4 cells (a) and a population of bone marrow cells (c), but not with thymocytes (b). Thin lines; control, thick lines; SM/C-2.6. B: Muscle satellite cells were stained with SM/C-2.6. Adult mouse muscle was stained with SM/C-2.6 (a, d), laminin (b), DAPI (c) (merged with a and b), M-cadherin (e), and DAPI (f) (merged with d and e). SM/C-2.6-reactive cells reside beneath the laminin layer and co-stained with anti-M-cadherin antibody. Single fibers from adult EDL muscle were stained with SM/C-2.6 (g), M-cadherin (h), and DAPI (merged with g and h) (i). SM/C-2.6-positive single cells attached to fibers were also stained with M-cadherin. SM/C-2.6 and M-cadherin-positive nuclei are distinguishable from myonuclei (i). Scale bars: 50 μm (a–i).

neonatal mouse muscle-derived mononuclear cells into SM/C-2.6-positive and -negative populations by using FACS sorting and cultured them in vitro. Neonatal muscle contains approximately 25% SM/C-2.6-positive cells (shown later, Fig. 4a). The positively and negatively sorted fractions contain more than 90% and less than 1% SM/C-2.6-positive

cells, respectively (data not shown). After 4 days of proliferating culture, the SM/C-2.6-positive fraction expressed MyoD, a typical myogenic transcription factor (Fig. 2a), while the negative fraction did not (Fig. 2d). The culture medium was then changed to differentiation medium, and the cells were cultured for an additional 7 days and examined for the expression of muscle-related molecules. Many myotubes were formed in the SM/C-2.6-positive fraction and were

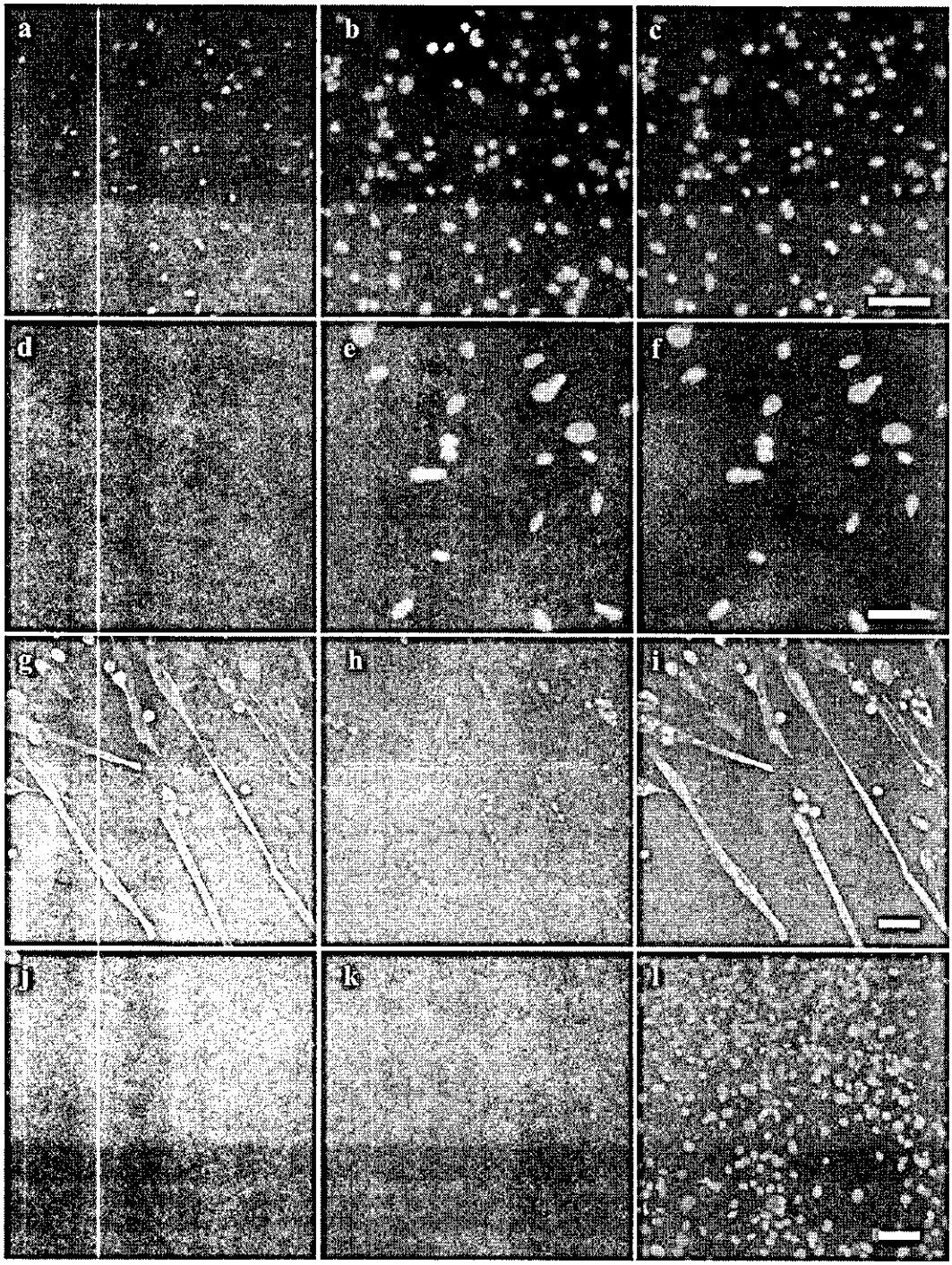

Fig. 2. SM/C-2.6-positive cells differentiate to myotubes in vitro. Freshly isolated single cells from neonatal (day 2) muscles were separated by their reactivity with SM/C-2.6. SM/C-2.6-positive cells compose approximately 25% of the cells in neonatal muscle. The positively and negatively sorted fractions contain 90% and 1% SM/C-2.6-positive cells, respectively. Positively (a–c) and negatively (d–f) sorted cells were cultured for 4 days under proliferating conditions, and the expression of MyoD was determined. Positively sorted cells became $MyoD^+$ (a). b and e; DAPI, c and f; merged. Positively (g–i) and negatively (j–l) sorted cells were then cultured for an additional 7 days under differentiating conditions. Positively sorted cells formed myotubes and became $desmin^+$ (g). Note that lines of $MyoD^+$ myonuclei formed in the newly generated myotubes (h). i and l, merged. Scale bars: 50 μm (a–i).

stained with desmin (Fig. 2g), a muscle-specific intermediate filament protein. MyoD-positive signals formed lines in the satellite cell-derived myonuclei of the myotubes (Fig. 2h), while no such structures were observed in the negative fraction (Figs. 2j–l). These results suggest that SM/C-2.6 specifically detects skeletal muscle satellite cells.

SM/C-2.6-positive cells differentiate into myofibers in vivo

We then examined the satellite cell activity of SM/C-2.6-positive cells in vivo. SM/C-2.6-positive cells were sorted from adult GFP-Tg mice, injected into the TA muscles of *mdx* mice, and the cryosections were examined 2 weeks after transplantation. The SM/C-2.6-positive fraction gave rise to several GFP-positive fibers (Figs. 3a and e), but the negative fraction did not (Figs. 3c and g). Then, we further confirmed that GFP-positive myofibers (Fig. 3i) were positive for dystrophin expression (Figs. 3j and k). Therefore, the SM/C-2.6-positive fraction includes satellite cells.

Age-related changes in SM/C-2.6-positive muscle satellite cells

SM/C-2.6-positive satellite cells were examined in C57BL/6 mice of different ages. Neonatal mice (postnatal day 2) contain approximately 25% satellite cells among the muscular mononuclear cells (Fig. 4a), and this amount declines with age: 13.1% at 4 weeks and 8.9% at 8 weeks of age (Figs. 4b and c). The results agree with earlier studies in which the number of satellite cells was seen to decline with age [13,36–38].

SM/C-2.6 detects neither M-cadherin nor c-met

The antigen recognized by SM/C-2.6 remains to be determined. As shown earlier (Figs. 1Bd and e), SM/C-2.6-positive cells co-express M-cadherin. C2/4 (C2C12) cells express both SM/C-2.6 and M-cadherin (Figs. 5a and b). To investigate whether SM/C-2.6 detects M-cad-

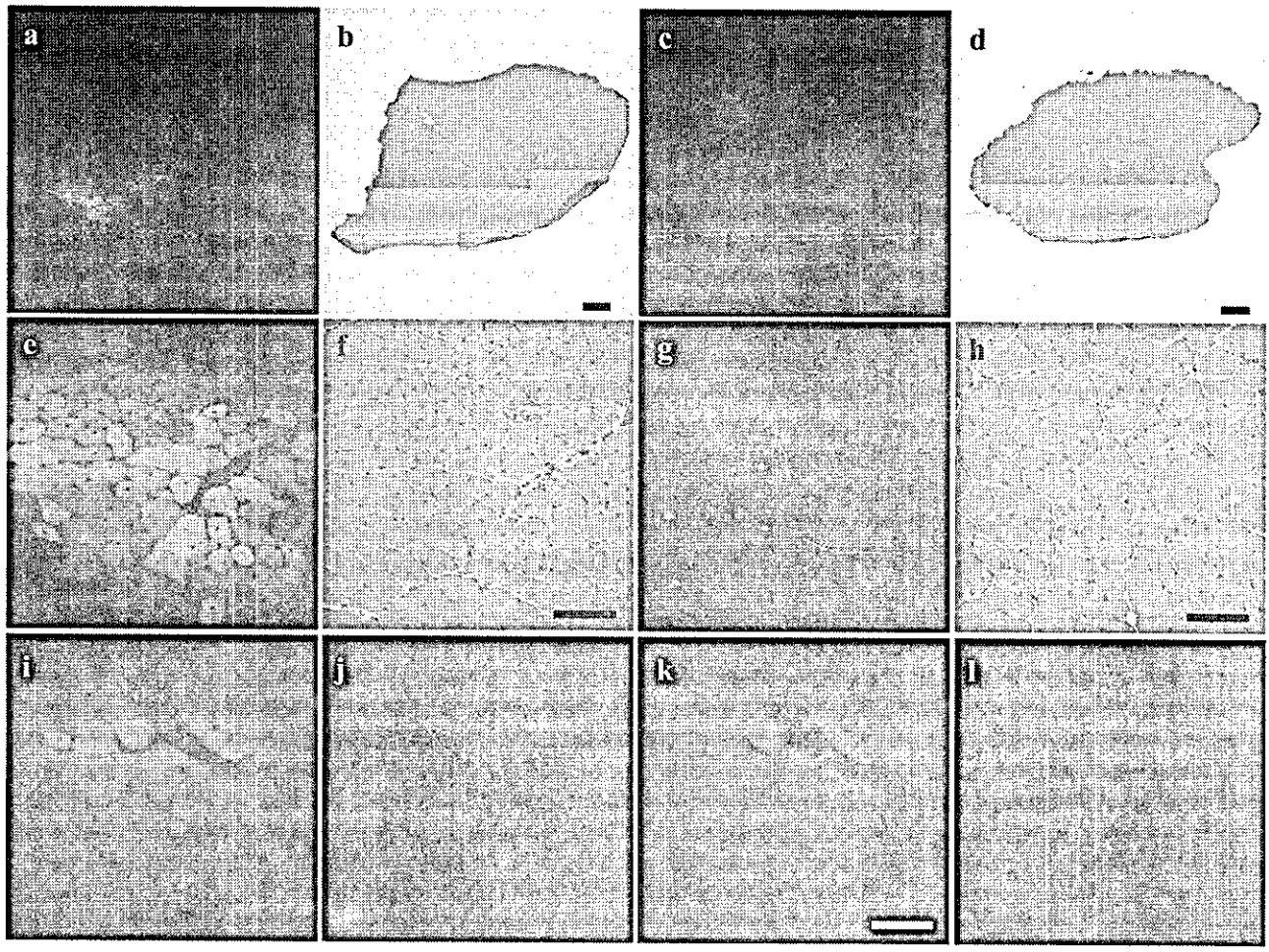

Fig. 3. SM/C-2.6-positive cells differentiate into myofibers in vivo. SM/C-2.6-positive and negative single cells from adult GFP-transgenic mice were obtained by cell sorting, and each muscle cell population was injected intramuscularly into the TA muscles of *mdx* mice. Two weeks later, muscles were isolated and cryosections were examined histologically (GFP: a, c, e, g, i, k; H–E: b, d, f, h). The positive fraction gave rise GFP^+ myofibers (a and e) with central nuclei, whereas the negative fraction did not (c and g). e–h, higher magnifications of a–d. GFP^+-myofibers (i) express dystrophin (j) (k, i and j were merged). GFP-negative area showed no dystrophin expression (l). Scale bars: 250 μm (a–d), and 50 μm (e–l).

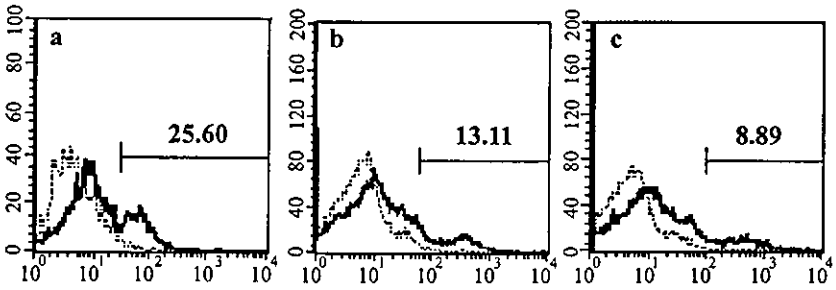

Fig. 4. Age-related changes in SM/C-2.6-positive satellite cells. Flow cytometric analyses of SM/C-2.6-positive cells in the muscles of mice at various ages. SM/C-2.6-positive cells in neonatal (day 2) thigh muscles (a), vastus lateralis and TA muscles from 4-week-old (b) to 8-week-old (c) mice are shown. The numbers of SM/C-2.6-positive cells decreases with age. The gates were set to exclude most of unstained cells. Percentages of unstained cells were equal in all panels.

herin, we compared SM/C-2.6 with M-cadherin expression in bone marrow cells. Approximately 10–15% of bone marrow cells express SM/C-2.6, but there are almost no SM/C-2.6/M-cadherin double positive cells (Fig. 5c). Similar to M-cadherin, we used flow cytometry to compare the expression of c-met and SM/C-2.6-reactive molecules on the mouse hepatocyte cell line NCTC1469. As shown in Fig. 5d, the NCTC1469 clone expresses c-met whereas it does not express SM/C-2.6-reactive molecules. The data definitively indicate that SM/C-2.6 detects neither M-cadherin nor c-met.

SM/C-2.6-positive cells express CD34 but not Sca-1, c-kit, or CD45

To investigate the expressions of several surface marker molecules on SM/C-2.6-positive cells, we analyzed adult muscle-derived mononuclear cells by flow cytometry. SM/C-2.6-positive cells did not co-express Sca-1, c-kit, or CD45 (Figs. 6a–c). However, all SM/C-2.6-positive cells (approximately 10% of muscle-derived mononuclear cells) co-expressed CD34 (Fig. 6d), and significant numbers of $CD34^+$ but SM/C-2.6-negative cells were also found.

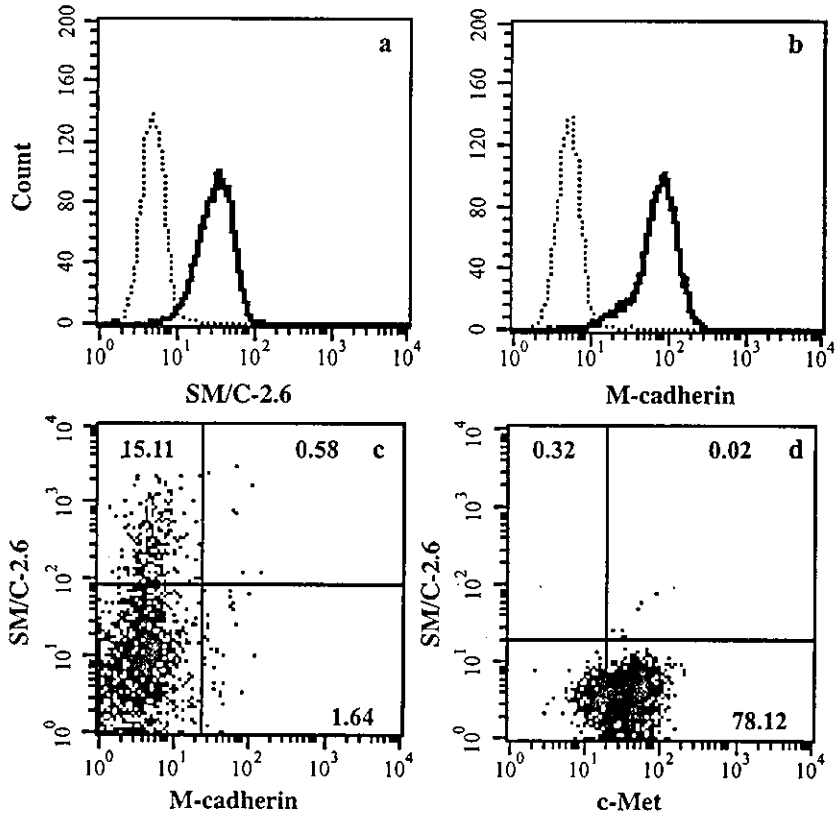

Fig. 5. SM/C-2.6 detects neither M-cadherin nor c-met. The SM/C-2.6-reactive molecule (a, c) and M-cadherin (b, c) are expressed on both C2/4 (a, b) and bone marrow cells (c). Two-color flow cytometry of bone marrow cells showed the SM/C-2.6-positive bone marrow cells do not express M-cadherin. A hepatocyte cell line, NCTC1469, expresses c-met but not the SM/C-2.6-reactive molecule (d). These data indicate that SM/C-2.6 detects neither M-cadherin nor c-met, which are known surface markers of satellite cells.

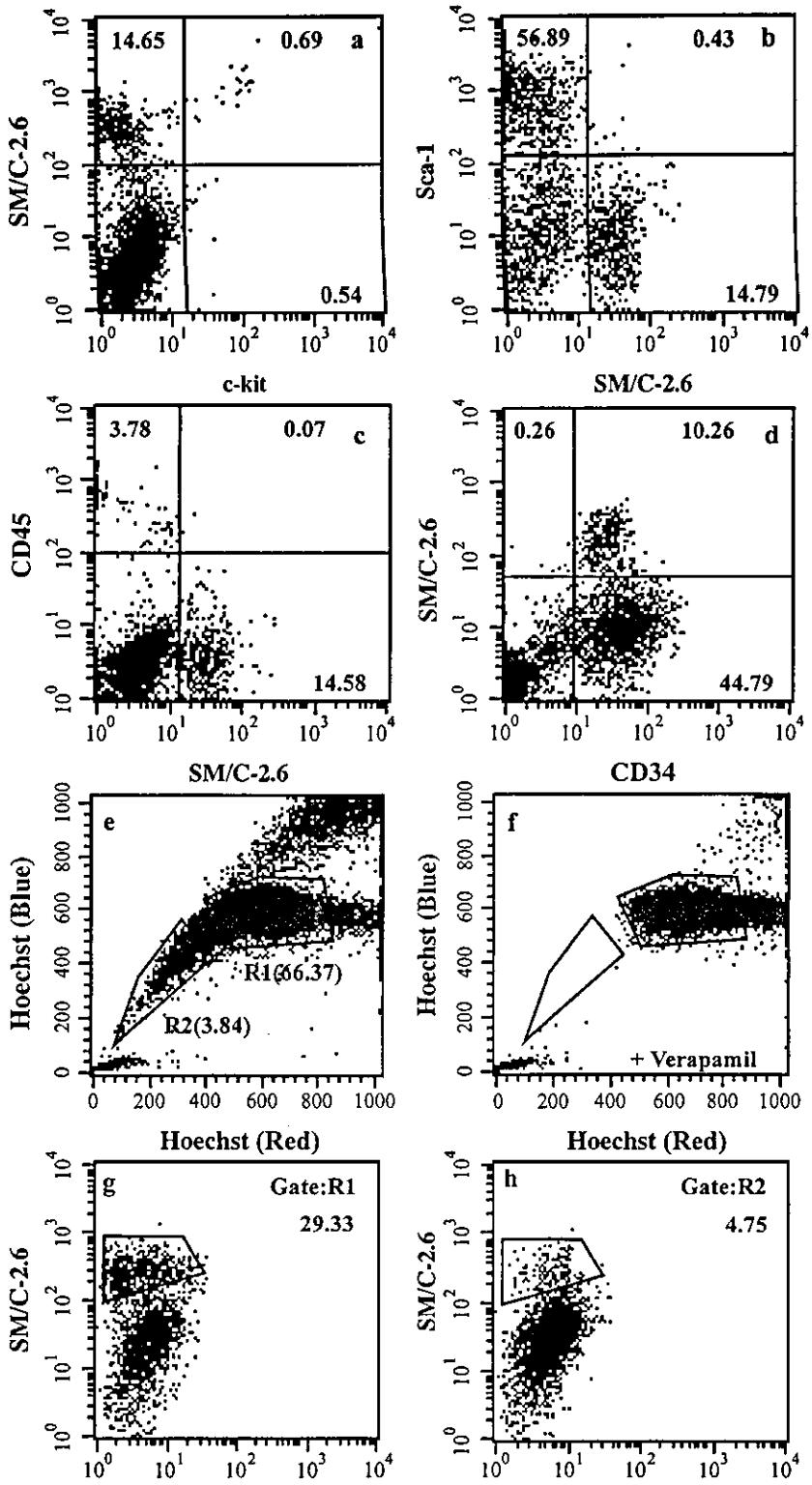

Fig. 6. Satellite cells are Sca-1$^-$, c-kit$^-$, CD45$^-$, CD34$^+$, and are included in the muscle MP fraction. Various surface markers on satellite cells were examined (a–d). SM/C-2.6-positive satellite cells are Sca-1$^-$ (a), c-kit$^-$ (b), CD45$^-$ (c), and CD34$^+$ (d). Muscle SP and MP fractions were separated by FACSVantageSE with (f) or without (e) verapamil. SM/C-2.6-positive cells among SP (3.84%) and MP (66.37%) cells were separated by flow cytometer. MP and SP include 29.33% (g) and 4.75% (h) SM/C-2.6-positive cells, respectively. This suggests that SM/C-2.6-positive satellite cells are mainly included in the muscle MP fraction.

Satellite cells are included in the fraction of muscle main population

Muscle-derived satellite cells can be isolated in the SP fraction by using the Hoechst-dye staining method, and the cells actively participated in myotube formation in the irradiated recipients [26]. Very recently, it was reported that hematopoietic stem cells from muscle SP are of hematopoietic origin [39]. On the other hand, muscle SP cells exhibit the potential to give rise to both myocytes and satellite cells after intramuscular transplantation [29]. We then investigated whether or not the SM/C-2.6-positive cells in adult skeletal muscle are found in the muscle SP fraction. As shown in Fig. 6e, muscle-derived mononuclear cells include 3% SP and a large number of MP cells. The SP fraction disappeared in cells treated with verapamil (Fig. 6f). The MP and SP fractions were gated (Fig. 6e, R1 and R2) and the SM/C-2.6-positive cells were examined. The gated MP fraction contained approximately 30% SM/C-2.6-positive cells (Fig. 6g) but the level was only 5% in the SP fraction (Fig. 6h). The results suggest that satellite cells are mainly included in the MP fraction.

Taken together, the results indicate that skeletal muscle quiescent satellite cells are Sca-1$^-$, c-kit$^-$, and CD45$^-$, but CD34$^+$, and are found in the muscle MP fraction.

Discussion

Muscle satellite cells are known as a key player in the skeletal muscle regeneration. Satellite cells are characterized by several significant features including histological location, electron micrographic characteristics in skeletal muscle, morphological change under physiological or pathological conditions, and the presence of a few specific marker proteins [14]. M-cadherin has been detected in the satellite cells of muscle [40]. Although several methods have been developed to isolate muscle satellite cells from enzymatically digested muscles [17–21], there is no definitive technique to isolate them from fresh muscle. In the present study, we aimed to purify skeletal muscle quiescent satellite cells using a mAb specific for them and to determine the surface phenotype. By immunizing rats with a C2/4 myoblast cell line (a subline of C2C12), we successfully established a novel mAb, SM/C-2.6, that detects muscle satellite cells by immunohistochemical and single fiber methods (Fig. 1B). By using FACS technique, we isolated SM/C-2.6-positive cells from mouse skeletal muscles and demonstrated that these cells differentiated into myotube or muscle fibers both in vivo and in vitro. SM/C-2.6-positive cells were detected in higher numbers in the neonatal muscle (postnatal day 2) than adult (4 week- or 8 week-old). This is consistent with earlier histological observations [14]. As shown in Figs. 2 and 3, FACS-sorted SM/C-2.6-positive cells became desmin$^+$ and MyoD$^+$ under proliferating or differentiating culture conditions. This is in good agreement with earlier studies that showed satellite cells become desmin$^+$ and MyoD$^+$ after muscle injury [41–44] or during short-term culture in vitro [45–47].

M-cadherin expression is restricted to satellite cells postnatally, and it is thought to be one of the proteins that define muscle satellite cells [40]. It is also known that hepatocyte growth factor activates quiescent skeletal muscle satellite cells in vitro [48], and that c-met, a receptor molecule for the factor, is expressed on quiescent satellite cells [49,50]. To investigate whether SM/C-2.6 detects these molecules, we compared the reactivity of SM/C-2.6 with the expressions of c-met in bone marrow cells or in a mouse hepatocyte cell line, NCTC1469. As clearly shown in Fig. 5, SM/C-2.6 detects neither M-cadherin nor c-met. Blanco-Bose et al. [51] reported that α7 integrin was useful for purification of myoblasts from cultured cells. However, α7 integrin is not likely the antigen recognized by SM/C-2.6 because α7 integrin is also expressed on myofibers [52–54]. We are now attempting to identify the reactive molecule.

Gussoni et al. [26] reported that muscle contains hematopoietic stem cells as well as muscle progenitor cells. Although the myogenic potential is highly enriched in muscle MP cells, SP cells with surface markers Sca-1$^+$, Lin$^-$, c-kit$^-$, CD45$^-$, and CD43$^-$, characterized from their efflux of Hoechst dye, are also incorporated into regenerated muscle fibers. The authors showed that the frequency of muscle progenitor cells is much lower than that of hematopoietic cells in muscle SP cells. McKinney-Freeman et al. [39] then showed that Sca-1$^-$ or CD45$^-$ cells give rise to donor-derived muscle fibers when they are injected into mouse muscle. Although it remains controversial, the data suggest that muscle-derived SP cells may not include sufficient muscle satellite cells. Rather, muscle SP cells are mainly composed of hematopoietic stem cells and differentiate into blood cells in the irradiated host. It is possible that they colonize in the muscle and differentiate into muscle satellite cells [29]. As described here, we have found that SM/C-2.6-positive cells in muscle MP cells, while SP cells contain few SM/C-2.6-positive cells. The results suggest that muscle quiescent satellite cells are a different population from SP cells of hematopoietic potential.

Sca-1 and c-kit are well-known surface markers of hematopoietic stem cells [55,56], and CD45 has been found in cells of hematopoietic origin but not on any non-hematopoietic cells [57]. CD34 is also known to be expressed on mouse hematopoietic stem cells [58,59]. As shown here, muscle-derived SM/C-2.6-positive cells do not co-express Sca-1, c-kit, or CD45 (Figs. 6a–c). On the other hand, all SM/C-2.6-positive cells (approximately 10% of muscle-derived mononuclear cells) co-express CD34 (Fig. 6d), and significant numbers of CD34-positive but SM/C-2.6-negative cells are also found. The expression of CD34 on SM/C-2.6-positive satellite cells is in agreement with earlier studies by Beauchamp et al. [60], in which they showed by a single fiber analysis that dormant satellite cells express

CD34 but not Sca-1 or CD45. The authors, however, reported in the paper that approximately 15–20% of satellite cells were negative for CD34 or M-cadherin staining, suggesting heterogeneity of satellite cells. The discrepancy in the CD34 expression on satellite cells remains to be investigated.

Because SM/C-2.6-negative cells give rise to few muscle fibers either in vitro or in vivo (Figs. 2 and 3), we conclude that SM/C-2.6 is a definitive marker of muscle satellite cells, which have the surface markers Sca-1$^-$, c-kit$^-$, CD45$^-$, and CD34$^+$. The characterization of the SM/C-2.6-reactive molecule will provide a powerful tool for understanding muscle-specific stem cell biology and helps us develop cell-base gene therapy or stem cell transplantation therapy for muscular dystrophies.

Acknowledgments

We thank Dr. M. D. Ohto for reading this manuscript. This work is supported by grants-in-aid from the Ministry of Health, Labor and Welfare of Japan.

References

[1] H.L. Aguila, K. Akashi, J. Domen, K. Gandy, E. Lagasse, R.E. Mebius, S. Morrison, J. Shizuru, S. Strober, N. Uchida, D.E. Wright, I.L. Weissman, From stem cells to lymphocytes: biology and transplantation, Immunol. Rev. 157 (1997) 13–40.

[2] H. Nakauchi, K. Sudo, H. Ema, Quantitative assessment of the stem cell self-renewal capacity, Ann. N. Y. Acad. Sci. 938 (2001) 18–24.

[3] R.F. Pereira, K.W. Halford, M.D. O'Hara, D.B. Leeper, B.P. Sokolov, M.D. Pollard, O. Bagasra, D.J. Prockop, Cultured adherent cells from marrow can serve as long-lasting precursor cells for bone, cartilage, and lung in irradiated mice, Proc. Natl. Acad. Sci. U. S. A. 92 (1995) 4857–4861.

[4] D.J. Prockop, Marrow stromal cells as stem cells for nonhematopoietic tissues, Science 276 (1997) 71–74.

[5] M.F. Pittenger, M. Mackay, A.S.C. Beck, R.K. Jaiswal, R. Douglas, J.D. Mosca, M.A. Moorman, D.W. Simonetti, S. Craig, D.R. Marshak, Multilineage potential of adult human mesenchymal stem cells, Science 284 (1999) 143–147.

[6] K.W. Liechty, T.C. MacKenzie, A.F. Shaaban, A. Radu, A.-M.B. Moseley, R. Deans, D.R. Marshak, A.W. Flake, Human mesenchymal stem cells engraft and demonstrate site-specific differentiation after in utero transplantation in sheep, Nat. Med. 6 (2000) 1282–1286.

[7] P. Bianco, P. Gehron-Robey, Marrow stromal stem cells, J. Clin. Invest. 105 (2000) 1663–1668.

[8] S. Makino, K. Fukuda, S. Miyoshi, F. Konishi, H. Kodama, J. Pan, M. Sano, T. Takahashi, S. Hori, H. Abe, J. Hata, A. Umezawa, S. Ogawa, Cardiomyocytes can be generated from marrow stromal cells in vitro, J. Clin. Invest. 103 (1999) 697–705.

[9] A. Erices, P. Conget, J.J. Minguell, Mesenchymal progenitor cells in human umbilical cord blood, Br. J. Haematol. 109 (2000) 235–242.

[10] C. Campagnoli, I.A. Roberts, S. Kumar, P.R. Bennett, I. Bellantuono, N.M. Fisk, Identification of mesenchymal stem/progenitor cells in human first-trimester fetal blood, liver, and bone marrow, Blood 98 (2001) 2396–2402.

[11] Y.A. Romanov, V.A. Svintsitskaya, V.N. Smirnov, Searching for alternative sources of postnatal human mesenchymal stem cells: candidate MSC-like cells from umbilical cord, Stem Cells 21 (2003) 105–110.

[12] A. Mauro, Satellite cells of skeletal muscle fibers, J. Biophys. Biochem. Cytol. 9 (1961) 493–495.

[13] R. Bischoff, The satellite cell and muscle regeneration, in: A.G. Engel, C. Franszini-Armstrong (Eds.), Myogenesis, McGraw-Hill, New York, 1994, pp. 97–118.

[14] M.J. Cullen, Muscle regeneration, in: S.C. Brown, J.A. Lucy (Eds.), Dystrophin: Gene, Protein, and Cell Biology, Cambridge Univ. Press, Cambridge, UK, 1997, pp. 233–273.

[15] M.D. Grounds, Towards understanding skeletal muscle regeneration, Pathol. Res. Pract. 187 (1991) 1–22.

[16] E. Schultz, Satellite cell proliferative compartments in growing skeletal muscles, Dev. Biol. 175 (1996) 84–94.

[17] R. Bischoff, Proliferation of muscle satellite cells on intact myofibers in culture, Dev. Biol. 115 (1986) 129–139.

[18] J.D. Rosenblatt, A.I. Lunt, D.J. Parry, T.A. Partridge, Culturing satellite cells from living single muscle fiber explants, In Vitro Cell. Dev. Biol. Anim. 31 (1995) 773–779.

[19] A. Baroffio, M. Hamann, L. Bernheim, M.L. Bochaton-Piallat, G. Gabbiani, C.R. Bader, Identification of self-renewing myoblasts in the progeny of single human muscle satellite cells, Differentiation 60 (1996) 47–57.

[20] A. Asakura, M. Komaki, M. Rudnicki, Muscle satellite cells are multipotential stem cells that exhibit myogenic, osteogenic, and adipogenic differentiation, Differentiation 68 (2001) 245–253.

[21] Z. Qu-Petersen, B. Deasy, R. Jankowski, M. Ikezawa, J. Cummins, R. Pruchnic, J. Mytinger, B. Cao, C. Gates, A. Wernig, J. Huard, Identification of a novel population of muscle stem cells in mice: potential for muscle regeneration, J. Cell Biol. 157 (2002) 851–864.

[22] S. Wakitani, T. Saito, A.I. Caplan, Myogenic cells derived from rat bone marrow mesenchymal stem cells exposed to 5-azacytidine, Muscle Nerve 18 (1995) 1417–1426.

[23] T. Saito, J.E. Dennis, D.P. Lennon, R.G. Young, A.I. Caplan, Myogenic expression of mesenchymal stem cells within myotubes of *mdx* mice in vitro and in vivo, Tissue Eng. 1 (1995) 327–343.

[24] G. Cossu, F. Mavilio, Myogenic stem cells for the therapy of primary myopathies: wishful thinking or therapeutic perspective? J. Clin. Invest. 105 (2000) 1669–1674.

[25] G. Ferrari, G. Cusella-De Angelis, M. Coletta, E. Paolucci, A. Stornaiuolo, G. Cossu, F. Mavilio, Muscle regeneration by bone marrow-derived myogenic progenitors, Science 279 (1998) 1528–1530.

[26] E. Gussoni, Y. Soneoka, C.D. Strickland, E.A. Buzney, M.K. Khan, A.F. Flint, L.M. Kunkel, R.C. Mulligan, Dystrophin expression in the *mdx* mouse restored by stem cell transplantation, Nature 401 (1999) 390–394.

[27] R.E. Bittner, C. Schofer, K. Weipoltshammer, S. Ivanova, B. Streubel, E. Hauser, M. Freilinger, H. Hoger, A. Elbe-Burger, F. Wachtler, Recruitment of bone-marrow-derived cells by skeletal and cardiac muscle in adult dystrophic *mdx* mice, Anat. Embryol. (Berl.) 199 (1999) 391–396.

[28] S. Fukada, Y. Miyagoe-Suzuki, H. Tsukihara, K. Yuasa, S. Higuchi, S. Ono, K. Tsujikawa, S. Takeda, H. Yamamoto, Muscle regeneration by reconstitution with bone marrow or fetal liver cells from green fluorescent protein-gene transgenic mice, J. Cell Sci. 115 (2002) 1285–1293.

[29] A. Asakura, P. Seale, A. Girgis-Gabardo, M.A. Rudnicki, Myogenic specification of side population cells in skeletal muscle, J. Cell Biol. 159 (2002) 123–134.

[30] T. Tamaki, A. Akatsuka, Y. Okada, Y. Matsuzaki, H. Okano, M. Kimura, Growth and differentiation potential of main- and side-population cells derived from murine skeletal muscle, Exp. Cell Res. 291 (2003) 83–90.

[31] M. Okabe, M. Ikawa, K. Kominami, T. Nakanishi, Y. Nishimune, 'Green mice' as a source of ubiquitous green cells, FEBS Lett. 407 (1997) 313–319.

[32] G.L. Hobbs, K.K. Sanford, W.R. Earle, V.J. Evans, Establishment of a clone of mouse liver cells from a single isolated cell, J. Natl. Cancer Inst. 18 (1957) 701–707.

[33] T.A. Rando, H.M. Blau, Primary mouse myoblast purification, characterization, and transplantation for cell-mediated gene therapy, J. Cell Biol. 125 (1994) 1275–1287.
[34] S. Nishikawa, M. Kusakabe, K. Yoshinaga, M. Ogawa, S. Hayashi, T. Kunisada, T. Era, T. Sakakura, S.-I. Nishikawa, In utero manipulation of coat color formation by a monoclonal anti-c-kit antibody: two distinct waves of c-kit-dependency during melanocyte development, EMBO J. 10 (1991) 2111–2118.
[35] A. Suzuki, Y. Zheng, S. Kaneko, M. Onodera, K. Fukao, H. Nakauchi, H. Taniguchi, Clonal identification and characterization of self-renewing pluripotent stem cells in the developing liver, J. Cell Biol. 156 (2002) 173–184.
[36] D.R. Campion, The muscle satellite cell: a review, Int. Rev. Cytol. 87 (1984) 225–251.
[37] R. Mazanet, C. Franzini-Armstrong, The satellite cell, in: A.G. Engel, B.Q. Banker (Eds.), Myology, vol. 2. McGraw-Hill, New York, 1986, pp. 285–307.
[38] G. Cossu, M. Molinaro, Cell heterogeneity in the myogenic lineage, Curr. Top. Dev. Biol. 18 (1987) 208–223.
[39] S.L. McKinney-Freeman, K.A. Jackson, F.D. Camargo, G. Ferrari, F. Mavilio, M.A. Goodell, Muscle-derived hematopoietic stem cells are hematopoietic in origin, Proc. Natl. Acad. Sci. U. S. A. 99 (2002) 1341–1346.
[40] A. Irintchev, M. Zeschnigk, A. Starzinski-Powitz, A. Wernig, Expression pattern of M-cadherin in normal, denervated, and regenerating mouse muscles, Dev. Dyn. 199 (1994) 326–337.
[41] T.R. Helliwell, Lectin binding and desmin staining during bupivicaine-induced necrosis and regeneration in rat skeletal muscle, J. Pathol. 155 (1988) 317–326.
[42] Y. Saito, I. Nonaka, Initiation of satellite cell replication in bupivacaine-induced myonecrosis, Acta Neuropathol. 88 (1994) 252–257.
[43] J. Rantanen, T. Hurme, R. Lukka, J. Heino, H. Kalimo, Satellite cell proliferation and the expression of myogenin and desmin in regenerating skeletal muscle: evidence for two different populations of satellite cells, Lab. Invest. 72 (1995) 341–347.
[44] G. Molnar, M.L. Ho, N.A. Schroedl, Evidence for multiple satellite cell populations and a non-myogenic cell type that is regulated differently in regenerating and growing skeletal muscle, Tissue Cell 28 (1996) 547–556.
[45] R.E. Allen, L.L. Rankin, E.A. Greene, L.K. Boxhorn, S.E. Johnson, R.G. Taylor, P.R. Pierce, Desmin is present in proliferating rat muscle satellite cells but not in bovine muscle satellite cells, J. Cell. Physiol. 149 (1991) 525–535.
[46] S.J. Kaufman, M. George-Weinstein, R.F. Foster, In vitro development of precursor cells in the myogenic lineage, Dev. Biol. 146 (1991) 228–238.
[47] S. Creuzet, L. Lescaudron, Z. Li, J. Fontaine-Perus, MyoD, myogenin, and desmin-nls-lacZ transgene emphasize the distinct patterns of satellite cell activation in growth and regeneration, Exp. Cell Res. 243 (1998) 241–253.
[48] R.E. Allen, S.M. Sheehan, R.G. Taylor, T.L. Kendall, G.M. Rice, Hepatocyte growth factor activates quiescent skeletal muscle satellite cells in vitro, J. Cell. Physiol. 165 (1995) 307–312.
[49] D.D. Cornelison, B.J. Wold, Single-cell analysis of regulatory gene expression in quiescent and activated mouse skeletal muscle satellite cells, Dev. Biol. 191 (1997) 270–283.
[50] L.A. Sabourin, A. Girgis-Gabardo, P. Seale, A.A. Sakura, M.A. Rudnicki, Reduced differentiation potential of primary MyoD−/− myogenic cells derived from adult skeletal muscle, J. Cell Biol. 144 (1999) 631–643.
[51] W.E. Blanco-Bose, C.C. Yao, R.H. Kramer, H.M. Blau, Purification of mouse primary myoblasts based on alpha 7 integrin expression, Exp. Cell Res. 265 (2001) 212–220.
[52] W.K. Song, W. Wang, R.F. Foster, D.A. Bielser, S. Kaufman, H36-alpha 7 is a novel integrin alpha chain that is developmentally regulated during skeletal myogenesis, J. Cell Biol. 117 (1992) 643–657.
[53] G. Collo, L. Starr, V. Quaranta, A new isoform of the laminin receptor integrin alpha 7 beta 1 is developmentally regulated in skeletal muscle, J. Biol. Chem. 268 (1993) 19019–19024.
[54] B.L. Ziober, M.P. Vu, N. Waleh, J. Crawford, C.S. Lin, R.H. Kramer, Alternative extracellular and cytoplasmic domains of the integrin alpha 7 subunit are differentially expressed during development, J. Biol. Chem. 268 (1993) 26773–26783.
[55] N. Uchida, I.L. Weissman, Searching for hematopoietic stem cells: evidence that Thy-1.1^{lo} Lin-Sca-1^{+} cells are the only stem cells in C57BL/Ka-Thy-1.1 bone marrow, J. Exp. Med. 175 (1992) 175–184.
[56] M. Osawa, K. Hanada, H. Hamada, H. Nakauchi, Long-term lymphohematopoietic reconstitution by a single CD34-low/negative hematopoietic stem cell, Science. 273 (1996) 242–245.
[57] I.S. Trowbridge, M.L. Thomas, CD45: an emerging role as a protein tyrosine phosphatase required for lymphocyte activation and development, Annu. Rev. Immunol. 12 (1994) 85–116.
[58] D.S. Krause, T. Ito, M.J. Fackler, M. Smith, M.I. Collector, S.J. Sharkis, W.S. May, Characterization of murine CD34, a marker for hematopoietic progenitor and stem cells, Blood 84 (1994) 691–701.
[59] D.S. Krause, M.J. Fackler, C.I. Civin, W.S. May, CD34: structure, biology, and clinical utility, Blood. 87 (1996) 1–13.
[60] J.R. Beauchamp, L. Heslop, D.S. Yu, S. Tajbakhsh, R.G. Kelly, A. Wernig, M.E. Buckingham, T.A. Partridge, P.S. Zammit, Expression of CD34 and Myf5 defines the majority of quiescent adult skeletal muscle satellite cells, J. Cell Biol. 151 (2000) 1221–1234.

Available online at www.sciencedirect.com

SCIENCE DIRECT

Molecular Brain Research 125 (2004) 1–12

MOLECULAR BRAIN RESEARCH

www.elsevier.com/locate/molbrainres

Research report

Identification and characterization of ε-sarcoglycans in the central nervous system☆

Akiyo Nishiyama[a,b], Takeshi Endo[b], Shin'ichi Takeda[a], Michihiro Imamura[a,*]

[a] *Department of Molecular Therapy, National Institute of Neuroscience, NCNP, 4-1-1 Ogawahigashi-cho, Kodaira, Tokyo 187-8502, Japan*
[b] *Graduate School of Science and Technology, Chiba University, Yayoi-cho, Inage, Chiba 263-8522, Japan*

Accepted 24 January 2004

Available online 30 April 2004

Abstract

α-, β-, γ-, and δ-Sarcoglycans (SGs) are transmembrane glycoprotein components of the dystrophin-associated protein (DAP) complex, which is critical for the stability of the striated muscle cell membrane. ε-SG was found as a homologue of α-SG, but unlike other SG members, it is ubiquitously expressed in various tissues as well as in striated muscle. Moreover, mutations in the ε-*SG* gene cause myoclonus-dystonia, indicating the importance of ε-SG for the function in the central nervous system. To gain insight into the role of ε-SG, its expression and subcellular distribution in mouse tissues and especially in the mouse brain were investigated. Analysis by reverse transcription-polymerase chain reaction showed four splice variants of ε-SG transcripts in the mouse brain, two of which are major transcript forms. One is a conventional form including exon 8 (ε-SG1), and the other is a novel form excluding exon 8 but including a previously unknown exon, 11b (ε-SG2). Immunoblot analysis using various mouse tissues indicated a broad expression pattern for ε-SG1, but ε-SG2 was expressed exclusively in the brain. Therefore, both ε-SG isoforms coexist in various regions of the brain. Furthermore, these isoforms were found in neuronal cells using immunohistochemical analysis. Subcellular fractionation of brain homogenates, however, indicated that ε-SG1 and ε-SG2 are relatively enriched in post- and pre-synaptic membrane fractions, respectively. These results suggest that the two ε-SG isoforms might play different roles in synaptic functions of the central nervous system.

Theme: Cellular and molecular biology
Topic: Gene structure and function: general

Keywords: ε-Sarcoglycan; Dystrophin-associated protein; Muscular dystrophy; Myoclonus-dystonia; Brain

1. Introduction

Sarcoglycans (SGs) are essential constituents of the dystrophin-associated protein (DAP) complex, a large, membrane-associated protein architecture that is critical for the integrity of striated muscle fibers. The DAP complex consists of many proteins, including syntrophins (α1, β1, and β2), dystrobrevins, dystroglycans (α and β), SGs (α, β, γ, and δ), and sarcospan, that directly or indirectly associate with dystrophin [13,42,48]. Dystrophin, an actin-binding cytoskeletal protein, associates with the muscle plasma membrane via β-dystroglycan, which in turn binds to α-dystroglycan. α-Dystroglycan tightly associates with the laminin-α2 chain, a major component of the basal lamina, indicating that the DAP complex links extracellular matrix to intercellular cytoskeletal actin. The dystrophin-DAP complex is thought to function in protecting the plasma membrane of striated muscle fibers from contraction-induced mechanical stress by linking the molecules [42,43].

α-, β-, γ-, and δ-SGs are membrane-spanning glycoproteins that comprise a subcomplex within the DAP complex and associate with the other membranous subcomplex, which is composed of α- and β- dystroglycans [49]. A defect in any one of these four SGs disrupts the entire SG complex in the striated muscle

☆ The cDNA sequences of mouse and human ε-SG2 have been submitted to the DDBJ (DNA Data Bank of Japan) with accession numbers AB117975 and AB117974, respectively.

* Corresponding author. Tel.: +81-42-346-1720; fax: +81-42-346-1750.
E-mail address: imamura@ncnp.go.jp (M. Imamura).

0169-328X/$ - see front matter © 2004 Elsevier B.V. All rights reserved.
doi:10.1016/j.molbrainres.2004.01.012

cell membrane and leads to limb-girdle muscular dystrophies [4,31,36,38,40,45]. Analyses of striated muscle of SG-deficient animals showed that the loss of a SG complex made the molecular interaction between α- and β- dystroglycans and between dystrophin and β-dystroglycan fragile [1,16,21]. These findings revealed that the SGs are functional only when they exist as a complex, and that they play a role in reinforcing the molecular linkage between the extracellular matrix and cytoskeletal actin. In addition to the structural role, the SG complex has been suggested to play a role in scaffolding for signal-transduction cascades, but its precise mechanism remains unknown [50]. Dystroglycans and the cytoplasmic members of DAPs, syntrophins and dystrobrevins, are expressed not only in muscle but also in various tissues, i.e., kidney, liver, lung, intestine and brain [3,35]. Recently, these proteins and dystrophin isoforms were shown to form complexes without SG complex in the central nervous system [8,37]. Little is known about their functional roles.

ε-SG, a type I transmembrane glycoprotein, was found as a homologue of α-SG [14,33]. In contrast to the expression of α-SG, which is specific to striated muscle, ε-SG is widely expressed in a variety of tissues including striated muscle, smooth muscle, lung, liver, kidney, spleen, testis, sciatic nerve, and brain [14,20]. ε-SG can form complexes with β-, γ-, and δ-SGs in skeletal [32] and smooth muscle cells [47] and with β- and δ-SGs in the Schwann cells surrounding peripheral nerve fibers [20]. Two ε-SG signals were detected in the brain by immunoblot analysis [14,20], but the localization and function of ε-SG have not been identified yet.

Recently, mutations in the human *ε-SG* gene have been shown to be associated with myoclonus-dystonia (M-D) [51]. M-D is a movement disorder characterized by rapid muscle contractions (myoclonus) and sustained twisting and repetitive movements, resulting in abnormal postures (dystonia). In addition to motor features, psychiatric symptoms, i.e., panic attacks, obsessive–compulsive behavior, or alcohol dependence, are reported in several M-D families [23,46]. These findings suggest that ε-SG has a key function in the central nervous system. Because a missense mutation in the *D2 dopamine receptor* gene is reportedly associated with M-D [23], it is intriguing to investigate the ε-SG expression in neuronal cells including dopaminergic neurons.

In this study, we found two ε-SG isoforms due to alternative splicing expressed in the mouse brain. One was an already reported conventional form; the other was a novel isoform specific to brain. Biochemical fractionation of mouse brains revealed that these two isoforms localized in different subcellular fractions. Furthermore, we clearly showed that the ε-SGs are broadly expressed in neuronal cells including dopaminergic neurons by immunocytochemical study. Our results provide the molecular basis for understanding the role of ε-SG in the central nervous system.

2. Materials and methods

2.1. Cloning of brain ε-SG cDNAs

The full-length mouse ε-SG cDNAs were amplified from a brain single-strand cDNA library (CeMines, Evergreen, CO, USA) by polymerase chain reaction (PCR) using the following set of oligonucleotide primers: 5′-GGAAAGGGTCGGGGGACACTC-3′ (nucleotide position, 19-39) and 5′-TGCGTAACCGATGTCAGGAAA-3′ (1392-1372) [14]. The amplification was carried out using LA-Taq polymerase (Takara Bio, Shiga, Japan) for 30 cycles, each cycle consisting of 94 °C for 1 min, 55 °C for 1 min, and 72 °C for 3 min.

The full-length human ε-SG cDNAs were obtained by reverse transcription-PCR (RT-PCR) using human cerebellum mRNA (Clontech, Palo Alto, CA, USA). The RT reaction was carried out with 1 μg of the poly A^+ RNA with a oligonucleotide reverse primer complementary to the sequence in the 3′-untranslated region of human ε-SG mRNA (5′-TCATGCATTATTGGAAGAGAAAA-3′, 1440-1418, [33]). The resulting single-strand cDNAs were used as the template for PCR amplification. The amplification was performed under the same conditions described above using a forward primer (5′-GTGCTTGGACGGGACAGG-GTC-3′, 77-97, [33]) in addition to the reverse primer used for the RT reaction (1440-1418).

The obtained full-length cDNAs of mouse and human were subcloned into a pCR2.1 vector (Invitrogen Life Technologies, Carlsbad, CA, USA), and the isolated clones were sequenced using an ABI377 sequencer (Applied Biosystems, Foster City, CA, USA). A homology search of the cDNA sequences (Genebank) was performed by using the online program 'BLAST the Mouse Genome' (NCBI; http://www.ncbi.nlm.nih.gov/genome/seq/MmBlast.html). A protein domains search of ε-SG was performed by using online software PROSITE (http://kr.expasy.org/site/support).

2.2. Structural analysis of ε-SG transcripts

Structural analysis of ε-SG transcripts was carried out in two steps, the RT-PCR to isolate full-length ε-SG from mouse tissues and the following nested PCR of the 3′-regions of the full-length cDNAs.

RT-PCR: Total RNA was prepared from 14 tissues of C57BL/6J adult mice, i.e., brain, heart, skeletal muscle, lung, pancreas, liver, kidney, spleen, small intestine, colon, testis, ovary, prostate and thymus, by use of TRIZOL reagent (Invitrogen Life Technologies). RT reactions were performed with 1 μg of the total RNA using a 21-mer oligonucleotide reverse primer complementary to a sequence in the 3′-untranslated region of mouse ε-SG mRNA (5′-TGCGTAACCGATGTCAGGAAA-3′, 1392-1372 [14]). The resulting amplified single-strand cDNAs were used as the template for PCR amplification. The PCR was carried out under the same conditions described above with the 21-

mer forward primer (nucleotide position 19-39 [14]). The PCR products were separated by electrophoresis on agarose gel (1% agarose), and the 1.4-kbp full-length ε-SG fragments were purified by Wizard® SV Gel and PCR Clean-Up System (Promega, Madison, WI, USA).

Nested PCR: The inclusion or exclusion of exon 8 and 11b was examined by nested PCR of the purified full-length ε-SG cDNAs using following primer sets: 5′-GCTTATATCATGTGCTGCCGA-3′ (976-996) and 5′-GGGCCATGCAATCTCTCTGTT-3′ (1119-1099) [14] for exon 8 and 5′-AACTACGACAGCACCAACATG-3′ (1183-1203) and 5′-GTGAGACACGGCTGCAGCAGT-3′ (1324-1344) [14] for exon 11b. Amplification of the long region containing both exons 8 and 11b was carried out using the above forward primer (976-996) for exon 8 and the reverse primer (1324-1344) for exon 11b. The resulting PCR products were separated by polyacrylamide gel (8%) electrophoresis and stained with ethidium bromide (EtBr). The EtBr signals were detected on image analyizer (Lumi-Imager™ F1; Roche Diagnostics, Penzsberg, Germany) and quantified using the computer software, Lumi-Analyst 3.1 (Roche Diagnostics).

Structural analysis of the 3′ region of human ε-SG transcripts was carried out by PCR using first strand cDNAs from brain, heart, skeletal muscle, lung, pancreas, liver, kidney, spleen, small intestine, colon, testis, ovary, prostate and thymus (Clontech) with primer sets: 5′-GCTTATATCATGTGCTGCCGA-3′ (1045-1065) and 5′-AGGGTGGAACACAGGAAGCGT-3′ (1215-1195) [33] for exon 8 and 5′-ACAGACAACTATGATAGCACA-3′ (1246-1266) and 5′-TTCAGTCAGTTTTCTTTCTTCAG-3′ (1372-1350) [33] for exon 11b. Amplification of the region containing both exon 8 and 11b was performed using the above forward primer (1045-1065) and the reverse primer (1372-1350).

2.3. Antibodies

Mouse monoclonal antibodies against SNAP-25, PSD-95, and eNOS were purchased from BD Transduction Laboratories (San Diego, CA, USA). The other mouse monoclonal antibodies, anti-synaptophysin and Cy3-conjugated anti-glial fibrillary acidic protein (GFAP) were purchased form Sigma (St. Louis, MO, USA).

A rat monoclonal antibody against laminin-α2 chain was purchased from Alexis Biochemicals (Laufelfingen, Switzerland). Affinity-purified sheep antibody against tyrosine hydroxylase (TH) and rabbit antibody against GFAP were purchased from Chemicon International Lab (Temecula, CA, USA).

Affinity-purified rabbit antibody against the whole cytoplasmic region of ε-SG (Esg-Cyt antibody) was newly generated for the present study by the same method as previously described [20].

Rabbit antibodies against unique COOH-terminal sequences of ε-SG variants were raised against GST-fusion proteins. The 3′-terminal short cDNA fragment was amplified from each full-length ε-SG cDNA, including or excluding exon 11b, by PCR using the following oligonucleotide primer sets: 5′-TCATGCATTATTGGAAGAGAAAA-3′ (1440-1418) and 5′-ACAGACAACTATGATAGCACA-3′ (1246-1266) [33] for the cDNA with exon 11b and 5′-TCATGCATTATTGGAAGAGAAAA-3′ (1440-1418) and 5′-CAGAACTTGCCACATCAGACT-3′ (1291-1311) [33] for the cDNA without exon 11b. The amplification was carried out using Pyrobest (Takara) for 30 cycles, each cycle consisting of 98 °C for 10 s and 60 °C for 30 s. The amplified DNA fragments were subcloned into the pCR-Blunt vector (Invitrogen), and then the *Eco*RI-fragments of ε-SG variants were purified from a cloned pCR-Blunt plasmid and ligated into a pGEX expression vector (Amersham Biosciences K.K., Tokyo, Japan). Recombinant proteins were expressed as a fusion protein with GST in *E. coli* and purified from the soluble fraction of cell lysates on a glutathione-sepharose column as previously described [20]. These recombinant proteins were used as antigens. The antisera obtained were purified using affinity columns coupled with two kinds of synthetic peptides, i.e., CTGDFRLTTFQRFEVNGIPEERKLTEAMNL (amino acids 399-427) for ε-SG including exon 11b (Esg-C2 antibody) and CGGTTGKWYP (amino acids 407-413 [33]) for the ε-SG excluding exon 11b (Esg-C1 antibody).

The antibody against the sequence encoded in exon 8 (Esg-E8 antibody) was purified from antiserum against the whole cytoplasmic region of ε-SG using an affinity column conjugated with the synthetic peptide, CGVEKRNMQTPDIQ (amino acids 321-333 [33]).

2.4. Fusion proteins

To examine the specific reactivity of the purified anti-ε-SG antibodies, cytoplasmic regions of ε-SG variants were generated as recombinant fusion proteins with GST.

Three kinds of cDNA fragment encoding cytoplasmic regions of ε-SG variants were amplified from full-length ε-SG cDNAs by PCR using the following oligonucleotide primers: 5′-GCTTATATCATGTGCTGCCGA-3′ (976-996 [14]) and 5′-GTGAGACACGGCTGCAGCAGT-3′ (1324-1344 [14]) for mouse ε-SG. The enzyme reaction, using Pyrobest (Takara), and expression and purification of GST-fusion proteins were carried out under the same experimental conditions described in "Antibodies".

2.5. Immunocytochemistry

Cryosections (14 μm) of mouse brain were used for immunofluorescence staining. The cryosections were mounted on slide glasses and fixed in cold acetone (−20 °C). After equilibration of the fixed sections with Tris-buffered saline (TBS), the sections were blocked in TBS containing 2% casein. Indirect immunofluorescence microscopy was performed as previously described [20], using the

following primary antibodies at appropriate dilutions: affinity purified Esg-Cyt rabbit antibody at 1:1000, anti-TH sheep antibody at 1:200, anti-laminin-α2 chain rat antibody at 1:100, and Cy3-conjugated anti-GFAP mouse antibody at 1:1000. As secondary antibodies, Alexa488-conjugated anti-rabbit IgG (1:600), Alexa568-conjugated anti-sheep IgG (1:1000), and Alexa568-conjugated anti-rat IgG (1:1000) antibodies (Molecular Probes, Eugene, OR, USA) were used. A fluorescent Nissl stain was performed using NeuroTrace 640/660 (Molecular Probes) according to the manufacturer's protocol. Fluorescence signals on cryosections were observed using a confocal laser scanning microscope (Leica TCS SP; Leica, Heidelberg, Germany).

2.6. Subcellular fractionation

Biochemical fractionation of mouse brain homogenate was performed as described by Huttner et al. [18] and Kahle et al. [22]. Cerebellum-excised mouse brains were homogenized in ice-cold Hepes buffer (4 mM Hepes-NaOH, pH 7.3, and a protease inhibitor cocktail, 0.5 mM PMSF) containing 320 mM sucrose using a Dounce homogenizer. The brain homogenate (H) was centrifuged at $1000 \times g$ to remove nuclei and large debris (P1). The supernatant (S1) was centrifuged at $12{,}500 \times g$ to obtain a crude synaptosomal fraction (P2) and subsequently lysed hypoosmotically and centrifuged at $25{,}000 \times g$ to pellet a synaptosomal membrane fraction (LP1). Then the resulting supernatant (LS1) was centrifuged at $165{,}000 \times g$ to obtain a synaptic vesicle-enriched fraction (LP2). Concurrently, the supernatant (S2) of the crude synaptosomal fraction (P2) was centrifuged at $165{,}000 \times g$ to obtain a cytosolic fraction (S3) and a light membrane/microsome-enriched fraction (P3; hereafter referred to as light membrane). A postsynaptic density fraction (PSD) was prepared by washing the LP1 with Hepes-buffered solution containing 1% TritonX-100 according to the method of Phillips et al. [44].

2.7. Other procedures

Purification of capillary endothelial cells was performed using BS-1 lectin beads according to the method of Da Silva-Azevedo et al. [9]. SDS-polyacrylamide electrophoresis (SDS-PAGE) and protein transfer to the PVDF membrane were performed as described by Laemmli [26] and Kyhse-Anderson [25], respectively. Immunoreactive protein bands in the immunoblotting were visualized using a chemiluminescence detection system (ECL; Amersham Biosciences K.K.). Protein concentration was determined using Protein assay (Bio-Rad Laboratories, Hercules, CA, USA) with bovine serum albumin as a standard. All animal handling procedures were in accordance with a protocol

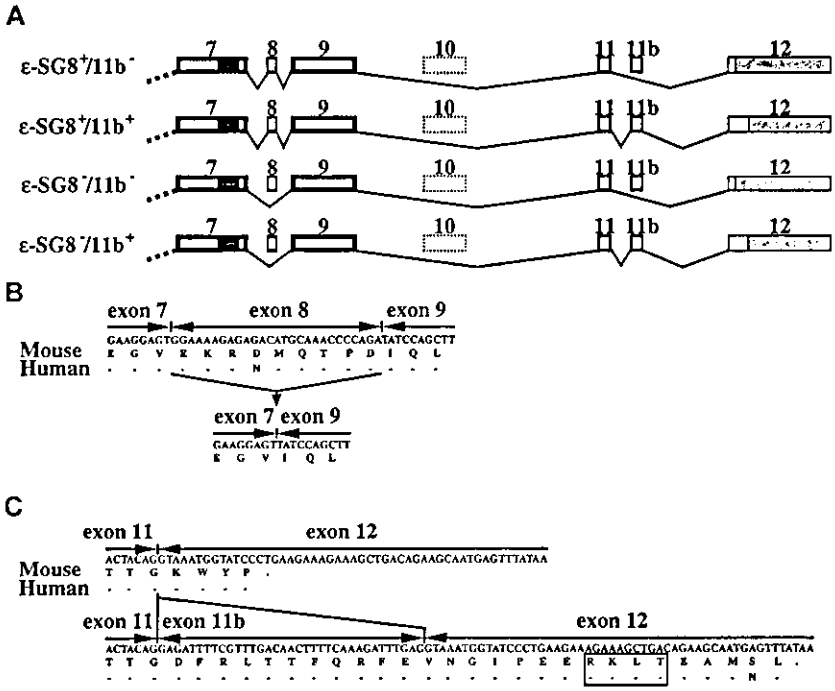

Fig. 1. Structures of ε-SG splice variants isolated from the mouse brain. (A) The exon organization of four ε-SG transcripts is schematically represented. Their 3′-terminal structures, corresponding to the region from exon 7 to exon 12, are shown. There was an alternative splicing around exon 8 and another alternative splicing around a newly found exon, 11b. The four resulting clones are designated ε-SG8$^+$/11b$^-$, ε-SG8$^+$/11b$^+$, ε-SG8$^-$/11b$^-$, and ε-SG8$^-$/11b$^+$. The black box in exon 7 indicates the region encoding the transmembrane domain. The shaded box in exon 12 indicates the untranslated region. The number of exons is given according to the human *SGCE* gene [33], although the sequence corresponding to exon 10 of the *SGCE* gene has not been found in the mouse genome database. (B) and (C) Represent the deduced amino acid sequences from the ε-SG variants without exon 8 and with the insertion of the newly found exon 11b, respectively. Identities between the mouse and human sequences are indicated by *dashes*. A possible site of phosphorylation by cyclic nucleotide-dependent protein kinases is boxed.

approved by the National Institute of Neurosciensce, NCNP, Japan.

3. Results

3.1. Identification of variants of ε-SG transcript in the brain

Previous immunoblot studies showed that ε-SG was widely expressed in a variety of mouse tissues as a 46 kDa protein. However, in the brain, signal(s) other than the 46 kDa ε-SG were detected [14,20]. This observation implies the possibility of a novel ε-SG isoform in the brain. To elucidate the presence of the brain-specific isoform of ε-SG, we searched for variants of ε-SG transcripts in the mouse brain.

We obtained cDNA clones having the entire coding region of ε-SG from mouse brain by RT-PCR. Analysis of their sequences showed that ε-SG transcripts were variable at two sites of the 3′ terminal region (Fig. 1). One variation is the inclusion or exclusion of exon 8, and the other is the inclusion or exclusion of a novel sequence between exon 11 and exon 12 (Fig. 1C). A homology search of the sequence in the mouse genomic database (Genebank) found the same sequence in intron 11 of the mouse ε-*SG* gene (*Sgce*), where splice-donor and -acceptor roles have been completely maintained (data not shown). Therefore, we numbered the new sequence as exon 11b, and the resulting four transcripts were designated as ε-SG8$^+$/11b$^-$, ε-SG8$^+$/11b$^+$, ε-SG8$^-$/11b$^-$ and ε-SG8$^-$/11b$^+$. In the primary structure, the exclusion of exon 8 is predicted to cause an in-frame deletion of 9 amino acids, while the inclusion of exon 11b causes the addition of 27 amino acids at the C-terminal (Fig. 1B,C). We also obtained the same results from human brain and the genomic database (Fig. 1). We numbered the exons and introns of *Sgce* according to a previous work on the human ε-*SG* gene (*SGCE*) [33].

Among the four ε-SG variants, one transcript that contains exon 8 but lacks exon 11b (ε-SG8$^+$/11b$^-$) has been already reported [14,33]. To clarify whether the exclusion of exon 8 and inclusion exon 11b occur specifically in the brain, we analyzed the 3′ structures of ε-SG transcripts in a variety of tissues. We initially amplified the full-length ε-SG transcripts from the tissues by RT-PCR and then performed second PCR with the same amount of full-length ε-SG cDNA to verify the presence of exon 8 or exon 11b. The second PCR, to verify whether transcripts have exon 8 or not, amplified the 144 bp fragment containing exon 8 from all tissues, but the 117 bp fragment lacking exon 8 was found mainly in brain, as shown in Fig. 2B. On the other hand, the PCR amplified the 197 bp-fragment containing exon 11b only from the brain, while the exon 11b-lacking 162 bp-fragment was amplified from all tissues examined.

Further, we performed RT-PCR analysis to clarify the combination of two alternative splicings, exon 8 and 11b. The sizes of PCR fragments comprising exon 8$^+$/11b$^-$, exon 8$^+$/11b$^+$, exon 8$^-$/11b$^-$ and exon 8$^-$/11b$^+$ were 369, 404, 342 and 377 bp, respectively. The 369- and 377-bp fragments were the major products in the brain and constituted 90% of the total product. The 369-bp fragment corresponded to a previously reported transcript, containing exon 8, but lacking

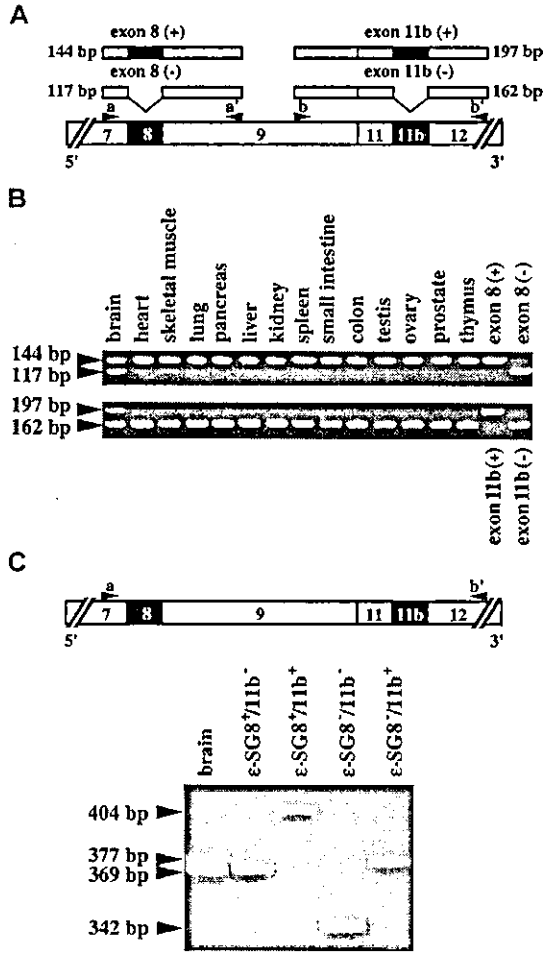

Fig. 2. Tissue expressions of splice variants of ε-SG transcripts. (A) Schematic representation of PCR products amplified from ε-SG splice variants. To examine the effects of alternative splicing of exon 8 and 11b on ε-SG transcripts in mouse various tissues, PCR analysis was performed using oligonucleotide primer sets (a and a′, and b and b′). The 3′-terminal structure of ε-SG, corresponding to a segment from exon 7 to the end of exon 12, is schematically represented at the bottom of the panel. (B) Expression of ε-SG splice variants in mouse tissues. First, cDNAs that cover the entire length of ε-SG were amplified from total RNAs of 14 different mouse tissues by RT-PCR. To analyze the inclusion or exclusion of exon 8 and exon 11b, respectively, a second PCR was performed using the primer sets described in (A) (a and a′, and b and b′). The resulting PCR products were separated by polyacrylamide gel (8%) electrophoresis. The 144 bp and 117 bp fragments in the upper panel indicate the inclusion or exclusion of exon 8. The 197 bp and 162 bp in the lower panel indicate the inclusion or exclusion of exon 11b. The right two lanes in each panel show the PCR products from the cloned ε-SG cDNAs including or excluding exon 11b and exon 8. (C) Combinations of the two alternative splicings were analyzed. First, cDNA that covers the entire length of ε-SGs was amplified from the mouse brain total RNA by RT-PCR, then the second PCR was performed using the primer set, a and b′, described in panel (A). The resulting DNA fragments are shown in the left lane as brain. The four right lanes indicate PCR products with the primer set using four cloned types of ε-SG cDNAs (see Fig. 1). The sizes of the PCR products comprising ε-SG8$^+$/11b$^-$, ε-SG8$^+$/11b$^+$, ε-SG8$^-$/11b$^-$ and ε-SG8$^-$/11b$^+$ were 369, 404, 342 and 377 bp, respectively.

exon 11b (ε-SG8$^+$/11b$^-$), while another 377-bp fragment was a novel transcript containing exon 11b, but lacking exon 8 (ε-SG 8$^-$/11b$^+$).

3.2. Identification of protein products from ε-SG transcripts

We generated three antibodies, Esg-C1, Esg-C2, and Esg-E8, that recognize variant-specific C-terminal structures

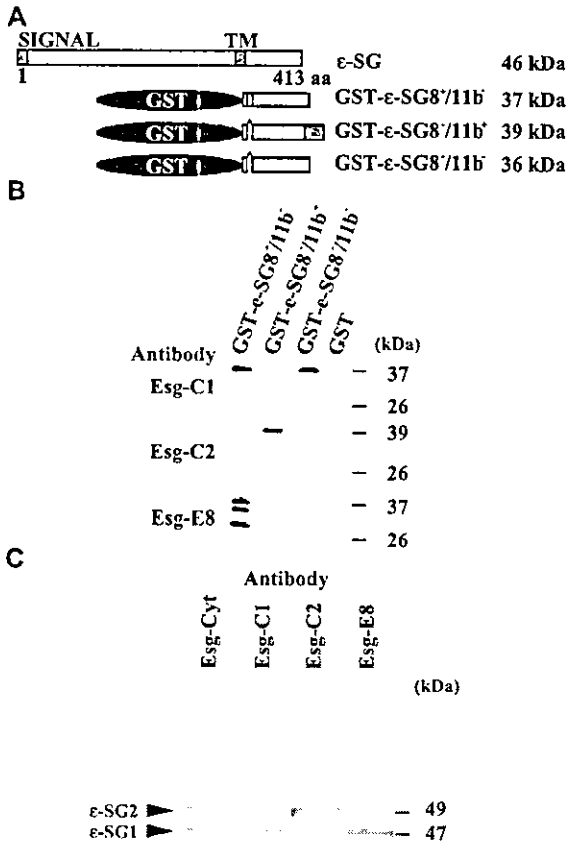

Fig. 3. Identification of protein products of ε-SG transcript variants in the mouse brain. (A) Schematic representation of GST-ε-SG fusion proteins that were used for testing immunoreactivities of antibodies, Esg-C1, Esg-C2, and Esg-E8. The shaded boxes in the N-terminal of ε-SG8$^+$/11b$^-$ and the C-terminal of ε-SG8$^-$/11b$^+$ indicate the peptide structures produced by the inclusion of exon 8 and exon 11b, respectively. (B) Specific reactivities of Esg-C1, Esg-C2, and Esg-E8 antibodies to ε-SG variants. Immunoblotting of GST-ε-SG-fusion proteins showed that Esg-C1 and Esg-C2 antibodies recognize the C-terminal of ε-SG excluding and including exon 11b, respectively. Esg-E8 was shown to recognize the ε-SG inclusion of exon 8. Note that Esg-E8 antibody recognizes degradation products of GST-ε-SG8$^+$/11b$^-$ protein. (C) Expression of two ε-SG isoforms in adult mouse brain. Ten micrograms of tissue lysate were separated on SDS-PAGE (9% polyacrylamide gel) and transferred onto polyvinylidene difluoride (PVDF) membranes. The membranes were sequentially treated with affinity-purified rabbit antibodies, Esg-C1, Esg-C2, and Esg-E8, and a horseradish peroxidase (HRP)-conjugated anti-rabbit secondary antibody. Immunostained bands were detected using a chemiluminescence detection system. The staining pattern of the antibody against the whole cytoplasmic region of ε-SG is shown in the left lane as Esg-Cyt.

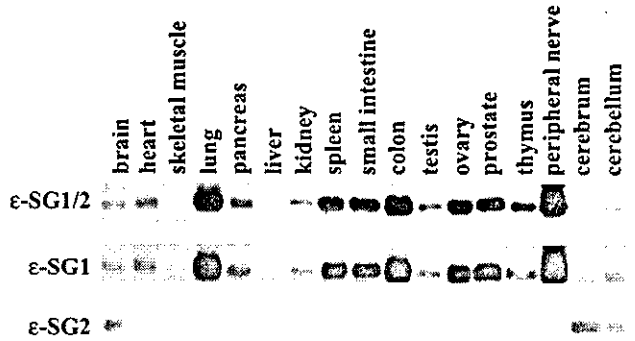

Fig. 4. Tissue expression of ε-SG1 and ε-SG2. Expression of the two ε-SG isoforms, ε-SG1 and ε-SG2, was examined in fifteen mouse tissues by immunoblotting. Ten micrograms of tissue lysates were separated on 9% SDS-PAGE and stained with the antibodies Esg-C1 and Esg-C2. The upper panel, indicated as ε-SG1/2, shows the staining pattern with Esg-Cyt antibody.

of ε-SG. Esg-C1 recognizes the C-terminal of ε-SG, which is the product of transcripts including exon 12, but lacking exon 11b. Esg-C2 recognizes the C-terminal of the other ε-SG, which is the product of transcripts including exon 11b and 12. Esg-E8 recognizes ε-SG, corresponding to transcripts that include exon 8 (Fig. 3B).

Immunoblotting of the mouse brain lysate with an antibody against the whole cytoplasmic region, Esg-Cyt, showed 47 and 49 kDa bands (Fig. 3C). Esg-C1 and Esg-E8 antibodies reacted to the 47 kDa band but not the 49 kDa, while Esg-C2 antibody reacted to the 49 kDa band but not the 47 kDa. These results indicated that two ε-SG isoforms are expressed mainly in the mouse brain. One is a conven-

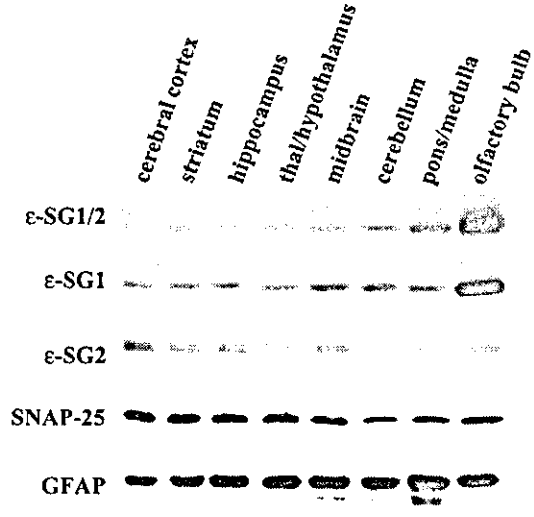

Fig. 5. Regional distribution of ε-SG1 and ε-SG2 in adult mouse brain. Adult mouse brains were separated into eight regions and homogenized in lysis buffer. These lysates were separated by SDS-PAGE (9% polyacrylamide gel) and immunostained with the antibodies Esg-C1 and Esg-C2. The upper panel (ε-SG1/2) shows the staining pattern with the Esg-Cyt antibody. The panels indicated as SNAP-25 and GFAP show the relative amounts of neuronal cells and astrocytes in each brain region. The thal/hypothalamus and pons/medulla indicate the regions including the thalamus and hypothalamus, and pons and medulla oblongata, respectively.

tional 47 kDa isoform derived from a transcript encoding exon 12 but not exon 11b, another is a novel 49 kDa isoform derived from a transcript encoding exon 11b, but not exon 8. We designated the former ε-SG1 and the latter ε-SG2.

The analysis of tissue expression with Esg-C1 and Esg-C2 antibodies showed that ε-SG1 was widely expressed in a variety of tissues, including brain, heart, skeletal muscle, lung, pancreas, liver, kidney, spleen, small intestine, colon, testis, ovary, prostate, thymus, peripheral nerve, while ε-SG2 was detected only in brain (Fig. 4).

3.3. Regional distribution of ε-SG1 and ε-SG2 in the mouse brain

We further examined the expression of the ε-SGs in eight regions of the mouse brain. Immunoblotting with Esg-C1 and Esg-C2 antibodies detected ε-SG1 and ε-SG2 in all regions examined: the cerebral cortex, striatum, hippocampus, thalamus/hypothalamus, midbrain, cerebellum, pons/medulla oblongata, and olfactory bulb (Fig. 5). The expression of ε-SG1 was more prominent in the olfactory bulb, while the expression of ε-SG2 was less abundant in the cerebellum, pons/medulla oblongata, and olfactory bulb.

3.4. Localization of ε-SG in the mouse brain

To identify the localization of ε-SGs, we performed immunocytochemical studies with the Esg-Cyt antibody. ε-SG immunoreactivity was clearly observed throughout the brain, but its signal is relatively high in olfactory bulb, cerebral cortex, hippocampus, pons, and cerebellar cortex (Fig. 6A). The ε-SG immunoreactivity partially overlapped

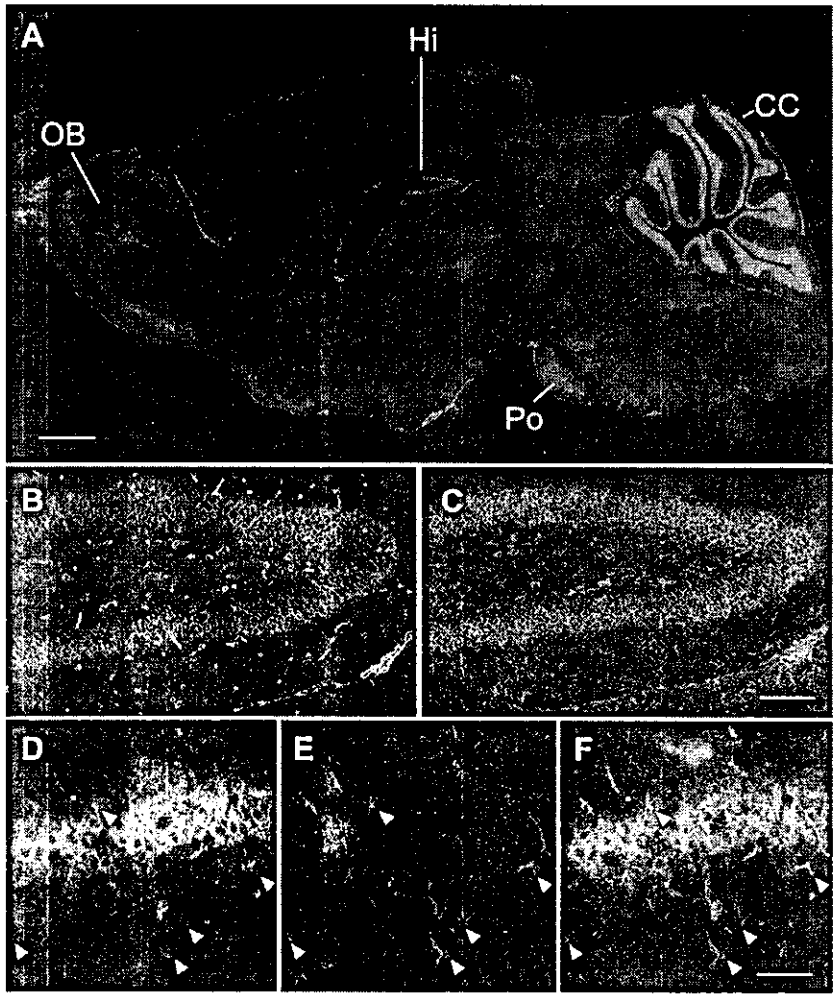

Fig. 6. Distribution of ε-SGs in adult mouse brain. Parasagittal cryosections of adult mouse brain were reacted with the Esg-Cyt antibody. The ε-SG immunoreactivity was visualized using Alexa488-conjugated secondary antibody (green). (A) Immunoreactivity of ε-SGs in a whole parasagittal section of mouse brain. The signals in the olfactory bulb (OB), hippocampus (Hi), pons (Po), and cerebellar cortex (CC) were intense. (B) and (C) Indicate the double-stain patterns of the dentate gyrus with Esg-Cyt rabbit antibody (green) and anti-lamini-α2 chain rat antibody (red) or Cy3-conjugated anti-GFAP mouse antibody (red), respectively. Note that the red fluorescence of lamini-α2 signals are seen as orange or yellow because of colocalization with the green signal of ε-SGs. (D–F) Higher magnification of a hippocampal CA2 region that was double-stained with Esg-Cyt (D) and Cy3-anti-GFAP antibody (E), and their merged image (F). Arrowheads indicate astrocytes showing immunoreactivity of ε-SGs. Scale bar = 1 mm for A, 100 μm for B and C, 50 μm for D–F. (For interpretation of the references to colour in this figure legend, the reader is referred to the web version of this article.)

with capillary vasculature stained with an antibody against laminin-α2 chain, a component of basal lamina surrounding micro-capillaries (Fig. 6B), whereas the localization of ε-SG was different from that of GFAP, a marker of astrocytes (Fig. 6C). In a higher magnification, however, a faint signal was detected in some astrocytes (Fig. 6D–F). Double-staining analysis with the Esg-Cyt antibody and fluorescent Nissl stain showed that ε-SGs expressed in neuronal cells within the olfactory bulb, hippocampus, pons, and cerebellar cortex, and localized along their cell bodies (Fig. 7). Furthermore, ε-SG immunoreactivity was detected in the cells expressing tyrosine hydroxylase (TH) within the sub-

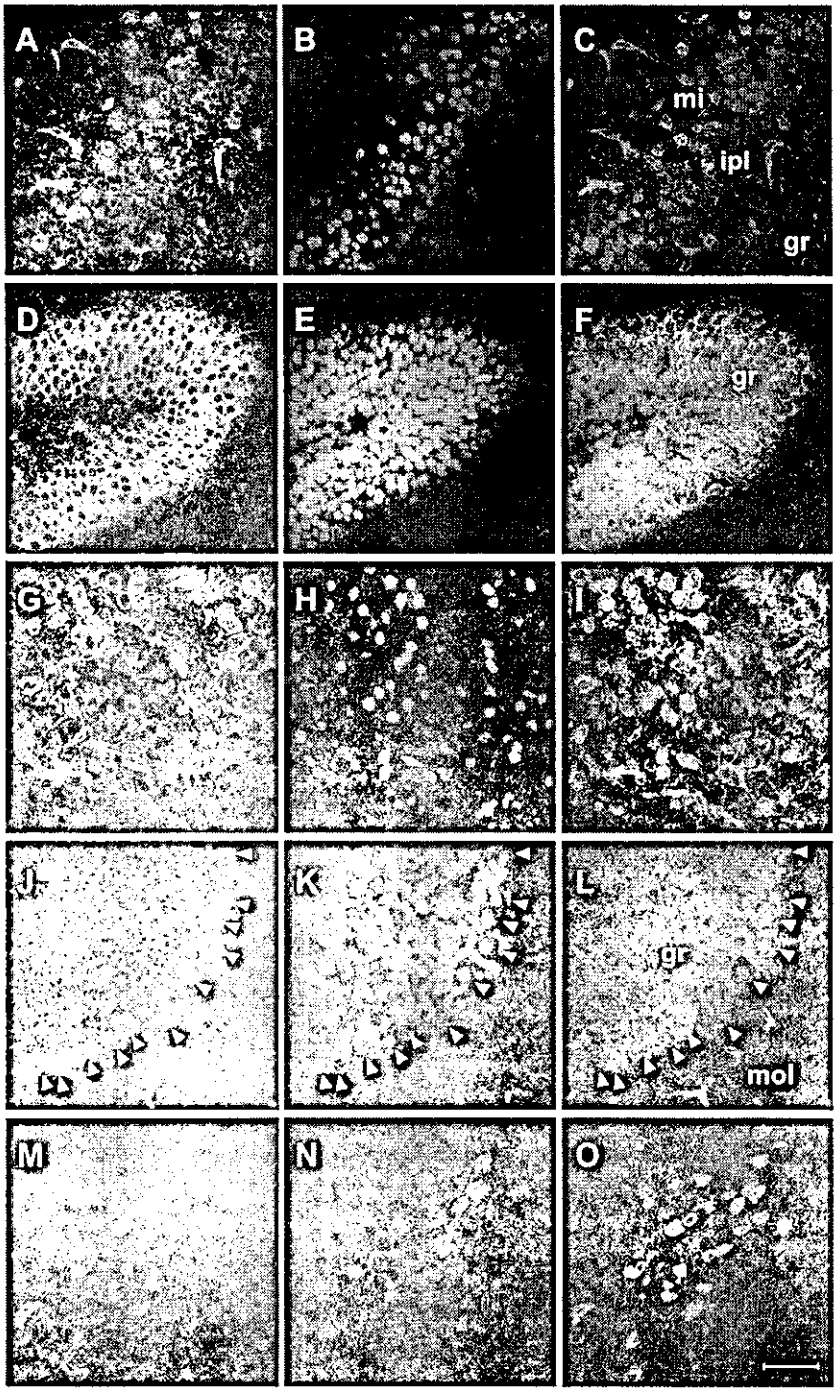

Fig. 7. Localization of ε-SGs in neuronal cells. Double-staining of mouse brain cryosections using Esg-Cyt antibody (A, D, G, J, M) and NeuroTrace™ fluorescent Nissl stain (B, E, H, K) was performed. The figures focus on the regions of the olfactory bulb (A–C), dentate gyrus (D–F), pons (G–I), and cerebellar cortex (J–L). In the staining of the substantia nigra (M–O), anti-TH sheep antibody was used instead of fluorescent Nissl stain and visualized by an Alexa568-secondary antibody (N). All the right-hand panels (C, F, I, L, O) are merged images of the two preceding panels. Arrowheads in panels J–L indicate Purkinje cells. mi, mitral cell layer; ipl, internal plexiform layer; gr, granular cell layer; mol, molecular cell layer. Scale bar = 50 μm.